

In-Service Evaluation of Temporary Sign Support Systems Against Wind Load

Caio Vitor Beojone
Nazmus Sakib Pallab
Yanfeng Ouyang

ICT Project R27-SP76

May 2026

ISSN: 0197-9191
ICT Series Report No. 26-007
<https://doi.org/10.36501/0197-9191/26-007>

TECHNICAL REPORT DOCUMENTATION PAGE

1. Report No. FHWA-ICT-26-007		2. Government Accession No. N/A		3. Recipient's Catalog No. N/A	
4. Title and Subtitle In-Service Evaluation of Temporary Sign Support Systems Against Wind Load				5. Report Date May 2026	
				6. Performing Organization Code N/A	
7. Authors Caio V. Beojone, https://orcid.org/0000-0002-6491-7104 Nazmus S. Pallab, https://orcid.org/0009-0009-8422-0433 Yanfeng Ouyang, https://orcid.org/0000-0002-5944-2044				8. Performing Organization Report No. ICT-26-007 UILU-2026-2007	
9. Performing Organization Name and Address Illinois Center for Transportation Department of Civil and Environmental Engineering University of Illinois Urbana-Champaign 205 North Mathews Avenue, MC-250 Urbana, IL 61801				10. Work Unit No. N/A	
				11. Contract or Grant No. R27-SP76	
12. Sponsoring Agency Name and Address Illinois Department of Transportation (SPR) Bureau of Research 126 East Ash Street Springfield, IL 62704				13. Type of Report and Period Covered Final Report 6/1/25–5/31/26	
				14. Sponsoring Agency Code	
15. Supplementary Notes Conducted in cooperation with the U.S. Department of Transportation, Federal Highway Administration. https://doi.org/10.36501/0197-9191/26-007					
16. Abstract This short study analyzes the performance of multiple temporary sign support systems under windy conditions and provides recommendations to the Bureau of Safety Programs and Engineering of the Illinois Department of Transportation (IDOT). The efforts included a literature review that summarizes past studies on the use of temporary sign support systems and the effects of winds on their structural integrity and stability as well as current practices on the use of such systems. Then, a set of field experiments were performed to test a list of temporary sign support systems under different natural and truck-generated wind loads, revealing critical conditions where they can fail. Finally, we extended a finite-element analysis to evaluate the structural impact of natural and truck-generated winds on selected sign support systems. Slow-ramping or longer-duration gusts produce greater sign deflections than short-duration gusts, and winds induced by a single truck or a three-truck platoon generate no significant sign deflection. These findings are summarized into deployment recommendations that account for the types of sign support systems and wind gust speeds. These recommendations will help IDOT make deployment decisions based on historical maximum gust speed data in each IDOT district per season.					
17. Key Words Sign Supports, Wind, Aerodynamic Force, Finite Element Method, Work Zone Traffic Control, Temporary Structures			18. Distribution Statement No restrictions. This document is available through the National Technical Information Service, Springfield, VA 22161.		
19. Security Classif. (of this report) Unclassified		20. Security Classif. (of this page) Unclassified		21. No. of Pages 39	22. Price N/A

ACKNOWLEDGMENT, DISCLAIMER, MANUFACTURERS' NAMES

This publication is based on the results of **ICT-R27-SP76: In-Service Evaluation of Temporary Sign Support Systems Against Wind Load**. ICT-R27-SP76 was conducted in cooperation with the Illinois Center for Transportation; the Illinois Department of Transportation; and the U.S. Department of Transportation, Federal Highway Administration.

Members of the Technical Review Panel (TRP) were the following:

- Juan Pava, TRP Chair, Illinois Department of Transportation
- Meiwu An, Illinois Department of Transportation
- Douglas Dirks, Illinois Department of Transportation
- Devon Holst, D2K Traffic
- Nick Lombardi, Federal Highway Administration
- Chad Morse, Illinois Department of Transportation
- Eric Murray, Warning Lites of Southern Illinois
- Nathan Peck, Illinois Department of Transportation
- Todd Schmidt, Federal Highway Administration
- Bill Seeman, RoadSafe Traffic Systems
- John Senger, Illinois Department of Transportation
- Jewell Stone, Illinois Department of Transportation
- Rachel Traficanti, Maintenance Coatings Company

The contents of this report reflect the view of the authors, who are responsible for the facts and the accuracy of the data presented herein. The contents do not necessarily reflect the official views or policies of the Illinois Center for Transportation, the Illinois Department of Transportation, or the Federal Highway Administration. This report does not constitute a standard, specification, or regulation.

Trademark or manufacturers' names appear in this report only because they are considered essential to the object of this document and do not constitute an endorsement of product by the Federal Highway Administration, the Illinois Department of Transportation, or the Illinois Center for Transportation.

EXECUTIVE SUMMARY

This study conducted a research analysis on the deployment performance of multiple temporary sign support systems. The purpose of this study was to provide recommendations to help the Bureau of Safety Programs and Engineering of the Illinois Department of Transportation (IDOT) establish engineering guidelines and policies on the deployment of these temporary sign support systems.

Three main tasks were included in this study. First, we conducted a literature review to investigate past studies on the use of temporary sign support systems and the effects of winds on their structural integrity and stability. We also reviewed current practices on the use of such temporary sign support systems. Second, a set of field experiments was performed to test several rigid and spring-based sign support systems under different wind loads. The field experiments recorded the response of sign support systems against the wind loads generated by a passing semitruck, fans, and natural winds. The tip deflection of selected spring-based sign support systems was connected to the wind gusts hitting their signs in real time. Third, the experimental results were replicated using finite-element analysis (FEA) on selected sign support systems. The workflow simulated transient aerodynamic loading on temporary sign support systems to compute their structural response under natural gusty winds and heavy vehicle-induced winds. Calculating wind forces and sign movement dynamically allowed us to estimate the overall deflection and tilt under time-varying wind conditions.

Some of the key findings are listed below:

- The literature review revealed that temporary sign support systems are required to satisfy two interrelated performance objectives: maintaining serviceability and legibility, while simultaneously meeting safety requirements when placed within work zones.
 - The process of installing temporary sign support systems is critical, especially deciding their position, securing them with ballasts, and ensuring that the surface is in order.
 - The quality of temporary sign support systems is multidimensional. Their durability and failure are determined by mechanical response and progressive damage during their life cycle, so it is important to evaluate their structural capacity and mechanical behavior.
- Field observations further demonstrated that the performance of temporary sign systems varied substantially among commonly used support types, revealing critical conditions where sign support systems can fail.
 - The design of temporary sign support systems had a central role in how they respond to winds, so these were organized into four groups depending on their height, number of legs, and use of springs.
 - Rigid temporary sign support systems (those without spring-based support) tended to fail under moderate winds but securing them with sandbags improved their resilience.

- Spring-based temporary sign support systems were less likely to fail, but sign visibility could be compromised if the springs are not stiff enough, due to large deflections from wind.
- Our preliminary analysis of the selected sign support systems showed the following:
 - Slow-ramping or longer-duration gusts produced greater deflection than short-duration gusts, because the structure had more time to build up displacement under sustained loading.
 - No significant deflection was observed from a single passing truck or even a three-truck platoon under no-wind conditions. However, results showed that vehicle pass-by loading may intensify sign oscillation when ambient wind gusts are already present.

These findings were summarized into deployment recommendations, where different types of temporary sign support systems were or were not recommended according to their performance under different wind speeds. For example, none of the tested temporary sign support systems are recommended when winds are 40 mph or faster. However, for scenarios with winds of 20 mph, all groups were deemed safe to deploy, with a note that rigid sign support systems must be properly secured. These recommendations were designed to be used in parallel with historical maximum gust speed data for each season in each IDOT district.

TABLE OF CONTENTS

CHAPTER 1: INTRODUCTION	1
CHAPTER 2: LITERATURE AND PRACTICE REVIEW	3
CHAPTER 3: FIELD EXPERIMENTS.....	6
TRUCK-GENERATED WINDS	7
Field Experiment Setup and Data Collection	8
Data Analysis.....	9
FAN-GENERATED WINDS	10
Experiment Setup and Data Collection.....	10
Data Analysis.....	11
NATURAL WINDS.....	12
Experiment Setup and Data Collection.....	12
Data Analysis.....	13
PROFILING OF WIND GUSTS AND SIGN TIP DEFLECTION.....	14
Experiment Setup and Data Collection.....	14
Data Analysis.....	15
CHAPTER 4: FINITE-ELEMENT ANALYSIS OF WIND-INDUCED STRUCTURAL RESPONSE OF TEMPORARY SIGN SUPPORT SYSTEMS	17
METHODOLOGY	17
3D Sign Stand Geometry Preparation.....	18
Computational Domain Definition.....	20
Material Properties and Model Assumptions.....	21
Transient Wind Simulation	22
Meshing Strategy	25
Load Transfer and Coupling Strategy.....	28
RESULTS.....	30
Response Under Natural Gusty Wind Conditions.....	31
Response to Vehicle-Induced Wind Loads.....	32
Serviceability-Based Interpretation	34

CHAPTER 5: RECOMMENDATIONS..... 36
REFERENCES..... 38

LIST OF FIGURES

Figure 1. Illustration. Expected maximum gust speeds in Illinois by season: (a) summer, (b) fall, (c) winter, and (d) spring. 7

Figure 2. Photo. Aerial photograph of ICART. 8

Figure 3. Schematic. ICART field experiments at (a) track separation, (b) cross-section of the track. 9

Figure 4. Photos. Selected frames from recorded videos of different tests: (a) beginning of test 1, (b) middle of test 2, and (c) end of test 3. Videos available at: ICART experiment videos. 10

Figure 5. Diagram. Position of the installed fans depending on the height of the tested sign support system. 10

Figure 6. Diagrams. Positioning of the recording camera and fans relative to the tested temporary sign support system. 11

Figure 7. Photos. Experimental setup using fans to generate artificial winds: (left) tall four-legged sign support system with springs, and (right) tripod sign support system. 12

Figure 8. Illustration. Position of recording camera and tested traffic sign stands. 13

Figure 9. Photo. Experimental setup to measure the profile of the wind causing deflections to a spring-based sign support system. 14

Figure 10. Graph. Recorded wind speeds during experiments with two sign stands. 15

Figure 11. Diagram. Flowchart of the numerical modeling framework. 18

Figure 12. Illustration. Structural models of temporary sign stands with different configurations in Autodesk Fusion 360. 19

Figure 13. Illustration. Computational fluid domain used for the fluid flow simulation in ANSYS Fluent 2025. 20

Figure 14. Photo and Illustration. Equivalent structural idealization of spring assemblies for finite-element modeling: (left) photo from field experiment; (right) model in ANSYS Mechanical 2025. 21

Figure 15. Photo and Illustration. Idealized fixed-base boundary conditions represent secured and ballasted conditions: (left) photo from field experiment; (right) model in Autodesk Fusion 360. 22

Figure 16. Graph. Synthetic gust profiles used for transient CFD inlet conditions. 22

Figure 17. Illustrations. Transient CFD visualizations of the flow field around the temporary sign support system in ANSYS Fluent 2025: (a) near-edge flow separation and vortex formation, and (b) downstream wake development in the sign’s lee region. 23

Figure 18. Illustrations. Heavy vehicle–induced aerodynamic gust simulations in ANSYS Fluent 2025: (a) single-truck pass-by scenario, and (b) three-truck platoon configuration. 24

Figure 19. Illustration. Unstructured hybrid Poly-Hexcore CFD mesh. (Left) Isometric view of the full fluid domain. (Right) Y-Z cross-sectional plane near the sign structure in ANSYS Mechanical 2025. ... 25

Figure 20. Illustration. Mesh deformation patterns around a moving body. 26

Figure 21. Illustration. Overset mesh configuration in ANSYS Fluent 2025: (a) schematic of the background air domain with an overlapping stationary sign region and a moving truck region; (b) fluid mesh distribution around the truck surfaces. 27

Figure 22. Illustrations. Structural finite-element mesh in ANSYS Mechanical 2025: (a) unstructured mesh with localized refinement near critical regions; (b) element quality distribution..... 28

Figure 23. Illustration. Instantaneous aerodynamic response of tilted temporary sign under wind loading: (a) velocity magnitude contours in the surrounding flow field; (b) static pressure contours on the sign surface..... 29

Figure 24. Illustration. Two-way coupling algorithm..... 30

Figure 25. Illustration. Geometric interpretation of sign tip displacement and tilting angle. 30

Figure 26. Graph. Time-displacement history plot of wind speed and sign tip displacement..... 31

Figure 27. Graph. (a) Time-displacement response, (b) displacement-wind speed response for different gust loading patterns..... 32

Figure 28. Graph. Pressure-time history and representative flow field at three characteristic instances of a single-truck pass-by event: (a) approaches, (b) passes alongside, and (c) moves away. 33

Figure 29. Graph. Time histories of tip displacement for the single-truck and three-truck platoon pass-by cases..... 34

Figure 30. Illustration. Transient oscillatory motion snapshots of the temporary sign during a single-truck pass by (10x scaled). 34

LIST OF TABLES

Table 1. List of Selected Temporary Sign Support Systems and Their Groups..... 6

Table 2. Summarized Beaufort Wind Scale 7

Table 3. Planned Experimental Scenarios..... 9

Table 4. Summary of Corrected Equivalent Tilting Angles for the Modeled Temporary Sign-Stand Configurations under Different Transient Aerodynamic Loading Conditions..... 35

Table 5. Summary of Recommendations..... 37

CHAPTER 1: INTRODUCTION

The state of Illinois accumulates more than 100 billion vehicle miles traveled annually on its roadway systems, much of which travel through hundreds of active work zones in the Illinois state highway system. The Illinois Department of Transportation (IDOT) has dedicated enormous efforts to provide safe, cost-effective, and sustainable mobility in Illinois in ways that enhance quality of life, promote economic prosperity, and protect the environment. IDOT has a strong interest in pursuing data-driven and science-based solutions to improve traffic efficiency and safety in Illinois' work zones.

During short traffic interventions (lasting less than three days), lightweight temporary signs and supports are becoming increasingly popular in work zones throughout the state. They are easy to install while providing drivers with crucial information to minimize serious injuries or property damage in case of a vehicle crash. Yet, industry has expressed concerns over the ability of new proprietary temporary sign stands to withstand field conditions such as wind loads. This is particularly an issue for Illinois, which is located on a very flat area with windy plains. As of May 25, 2025, there are 3,816 wind turbines in Illinois, which makes Illinois the fourth highest state in the nation in wind turbine installments (Choose Energy, 2026). As such, temporary traffic signs in Illinois work zones are frequently knocked down by high winds throughout the year. Furthermore, some sign and support designs are too light or too flexible to resist even wind loads generated from passing traffic such as trucks. Wind could knock down the signs or reposition them—resulting in degraded visibility which in turn could increase the risk of tort liability and traffic crashes. This has been a major issue in peer states as well.

Failure of sign support systems not only results directly in significant numbers of fatalities, injuries, and economic loss to motorists, but also increases IDOT workers' exposure to the additional need for resetting signs or tasks outside of sign deployment guidance (by anchoring the stands with ballasts). Hence, a thorough and objective study that evaluates the deployment performance of multiple temporary sign support systems is needed to help IDOT determine if deployment of such systems is feasible.

This study aims to conduct a research analysis on the deployment performance of multiple proprietary MASH-compliant temporary sign support systems. It will provide recommendations to IDOT's Bureau of Safety Programs and Engineering to help establish engineering guidelines and policies on their deployment. To accomplish this, specific research efforts of this study include the following:

- Conduct a literature review on temporary sign support systems, including their function, equipment, and components as well as deployment on various types of projects.
- Conduct experimental/observational research at existing test tracks (e.g., the ICART facility and parking lots in Rantoul, Illinois) on the rigidity, stability, and feasibility of temporary sign stands against front-facing wind.
- Build a preliminary finite-element analysis that quantifies the impacts of front-facing wind loads and that of a passing truck on selected temporary sign support systems.

The remainder of this report is organized as follows. Chapter 2 expands the literature review on the use of temporary traffic sign stands and the effects of winds on their structure, stability, and life-cycle, and it includes current practices on the use of such traffic control instruments. Chapter 3 describes the set of field experiments designed to test several temporary traffic sign stands under different natural and artificial wind loads. In Chapter 4, the results of the field experiments are replicated using finite-element analysis on selected stand designs and extend the analysis to evaluate the impact of passing trucks. Finally, Chapter 5 uses the previous results to provide recommendations and guidelines for IDOT.

CHAPTER 2: LITERATURE AND PRACTICE REVIEW

Per guidance of the Technical Review Panel, a literature review and synthesis were conducted to summarize the current state of practice of using temporary sign support systems in Illinois and peer states. It also documented findings associated with the safety of temporary sign support systems. The review primarily included manuals, research reports, and guidelines from peer states' departments of transportation (DOTs).

Traffic signs are highly susceptible to wind loading, and even moderate winds (10–30 mph) can accelerate deterioration through wind-induced vibration and excessive deflection (Toy et al., 1996). Under more extreme weather conditions, the resulting damage can occur at a large scale. For example, approximately 56,000 street signs were replaced in Miami-Dade County following the 2005 hurricane season, while more than 2,000 signs and signals were reportedly damaged during Hurricane Ike in Houston in 2008 (Center for Urban Transportation Research, 2007; Weatherford, 2008). Such damage has direct safety implications when signs are displaced, missing, or no longer capable of providing effective driver guidance. Based on a National Highway Traffic Safety Administration crash-causation survey, $3\% \pm 2.5\%$ of on-road crashes were attributed to sign or signal failure within the category of environmental-related causes (NHTSA, 2015). Similarly, in Texas, traffic-control sign support failures were reported to contribute to approximately 22,500 crashes annually during the 2014–2016 period (Texas Department of Transportation, 2016). In addition to safety concerns, wind-related damage imposes substantial maintenance and recovery costs. For instance, post-hurricane recovery estimates included approximately \$5 million in transportation system repairs associated with traffic signs and related traffic-control devices (Center for Urban Transportation Research, 2007).

These concerns are particularly evident in work zones, where temporary traffic control measures are required to protect both motorists and construction crews amid altered roadway conditions. Therefore, state DOTs typically provide guidance for the selection and deployment of temporary sign supports based on work zone duration and roadside exposure conditions. The *Manual on Uniform Traffic Control Devices (MUTCD)* distinguishes long-term stationary work—defined as work occurring at one location for more than three consecutive days—from shorter-duration operations. Long-term stationary work generally uses post-mounted warning signs, whereas shorter-duration work zones more commonly rely on portable sign supports. In both cases, supports located within the clear zone are expected to satisfy crashworthiness requirements (AASHTO, 2016). Existing guidance further emphasizes the importance of stability and maintenance. Portable signs that are prone to movement under wind loading should be supported adequately, and if stable and visible signing cannot be maintained, work activities may need to be suspended temporarily to preserve required visibility and driver guidance (Qiao et al., 2019). The *MUTCD* also provides installation-related criteria, including mounting height, sign orientation, and ballast considerations, to improve resistance to wind effects (FHWA, 2023). These principles are reinforced in state-level practice. For example, the Connecticut DOT recommends that construction zone signs be fastened securely to minimize wind-induced displacement and that periodic inspections be performed to verify continued compliance with specifications (CTDOT, 2017). Likewise, the Washington State DOT provides detailed installation

requirements, including embedment-depth guidance for sign supports, to improve resistance to wind loads acting on the sign face (WSDOT, 2015).

Temporary sign support systems used in practice vary substantially in form and performance. Work-zone guidance commonly distinguishes between embedding (anchored) signs and skid-mounted signs, with embedding systems often recommended in higher-wind regions (e.g., 70–90 mph) based on field observations and finite-element analysis (FEA) comparisons (Qiao et al., 2019). However, these recommendations also acknowledge that real-world stability depends on factors beyond steady wind demand alone, including vehicle-induced aerodynamic effects, strong localized wind forces, and roadway cross-slope or ground inclination. Consequently, field observations and simulation results must be interpreted together when assessing performance (Qiao et al., 2019). Experimental investigations of vehicle-induced gusts have shown that passing vehicles generate characteristic unsteady load pulses on sign panels. For overhead signs, the peak horizontal load frequently occurs opposite the direction of vehicle travel when the leading edge of the vehicle passes near the sign structure (Sanz-Andrés et al., 2003). Similarly, road-train vehicles traveling at 62 mph have been shown to generate local wind speeds up to 8 m/s (approximately 20 mph) near a sign, which approaches the threshold at which a rigid sign may become unstable (Kumar et al., 2023). Sign orientation relative to the roadway is also a critical parameter, as signs oriented perpendicular to the direction of traffic experience different peak load magnitudes, directions, and timing than signs aligned parallel to the roadway (Sanz-Andrés et al., 2003). From an operational perspective, a traffic sign with a tilting angle of 15 degrees from the vertical axis is commonly regarded as having failed in service (Center for Urban Transportation Research, 2007). Moreover, aeroelastic analyses indicate that sign-panel flexibility can produce multiple trailing load and oscillation cycles after a vehicle passes, thereby increasing fatigue demand under repeated loading (Barrero-Gil & Sanz-Andrés, 2009). Accordingly, structural damping is beneficial, particularly in reducing fatigue-related effects associated with repeated vehicle-induced excitation (Barrero-Gil & Sanz-Andrés, 2009).

To support design and evaluation, engineering assessments of temporary sign support systems increasingly rely on FEA to quantify wind-induced structural demand and compare alternative support configurations prior to field implementation. For example, Texas DOT's high-wind work-zone study evaluated multiple temporary sign types under several wind speeds (e.g., 40–90 mph) intended to represent realistic wind-demand scenarios. The reported FEA outputs included minimum safety factors, maximum pressure or stress, maximum displacement, and deviation angle (α) for each sign configuration (Du et al., 2020; Qiao et al., 2019). In addition to global structural response, material properties and connection behavior play a critical role in wind performance, particularly for portable roll-up sign systems, where failures frequently occur due to combined torsion and bending at the base of the vertical batten. Laboratory torsion and combined torsion-bending testing demonstrated that the governing failure mechanism was progressive cracking at the fiber-matrix interface, indicating that degradation may accumulate incrementally rather than occurring as an abrupt fracture event. From a serviceability standpoint, wind speeds of approximately 45 mph may cause a roll-up sign to fold and become unreadable, while strong crosswinds may rotate the sign away from approaching drivers. These findings underscore the importance of improving both weak-axis bending stiffness and torsional stiffness in critical structural members (Bae et al., 2014).

Overall, the literature indicates that temporary sign support systems must maintain acceptable field performance under wind and vehicle-induced gust loading while also meeting crashworthiness requirements when placed within the clear zone. However, current practice still lacks quantitative, system-level guidance that directly relates wind exposure to expected deflection and force response (Qiao et al., 2019; Du et al., 2020). Accordingly, the present study develops an FEA-based evaluation framework to compare temporary sign support systems under representative wind-loading scenarios and to quantify deflection angles and force demands that may inform future deployment guidance.

CHAPTER 3: FIELD EXPERIMENTS

Based on the literature and practice review, as well as recommendation of the TRP, we evaluated the list of temporary sign support systems in Table 1 via field experiments against natural and artificial winds. In order to maintain an anonymous evaluation of the selected temporary sign support systems, they were grouped according to their features, such as the number of legs, height, and use of wind-deflecting springs. In later analysis, tested temporary sign support systems are referred to by their group, instead of their codes, ensuring an anonymous evaluation.

Table 1. List of Selected Temporary Sign Support Systems and Their Groups

Code	Device Description	Material	Height to Bottom of Sign	Group
WZ-461	SZ-412X w/ Aluminum Sign	Aluminum	12 in.	Short four-legged without springs
WZ-462	SZ-484-2S w/ Aluminum Sign	Aluminum	84 in.	Tall four-legged with springs
WZ-450	Apex Summit w/ Aluminum Sign	Aluminum	84 in.	Tall four-legged with springs *
WZ-453	4860M Sign Stand w/ 48" × 48" Aluminum Sign	Aluminum	60 in.	Tall four-legged with springs
WZ-397	4860M-84 WindMaster Sign Stand	Aluminum	84 in.	Tall four-legged with springs
WZ-427	Plasticade SS621A Sign Stand w/ Aluminum Sign Panels at 84"	Aluminum	84 in.	Tall four-legged with springs
WZ-385	Big Buster Sign Stand	Aluminum	60 in.	Tall four-legged with springs
WZ-399	MDI Worldwide 50SM-2S Sign Stand Aluminum	Aluminum	12 in.	Short four-legged with springs
WZ-355	Plasticade SS420 Sign Stand System w/ 1S 48" × 48" Aluminum Sign	Aluminum	18 in.	Short four-legged with springs
WZ-384	Little Buster Sign Stand w/ Rigid Sign	Aluminum	18 in.	Short four-legged with springs
WZ-448	Eastern Metal of Elmira, Inc. Apex Tripod	Galvanized Steel	14 in.	Tripod
WZ-350	Watchdog SS105 Sign Stand	Powder Coated Steel	14 in.	Tripod

* This sign support system has a dual-leaf spring system that differs from the coil springs used in other sign support systems in this group.

We conducted experiments that cover two types of wind: natural wind and wind generated by passing traffic (i.e., artificial). The strength of natural wind is often measured by the Beaufort Scale, as shown in Table 2. For natural wind experiments, we targeted days with moderate and high winds (Beaufort Scales of 5–6 and 7–8, respectively). Artificial winds, especially by heavy-duty vehicles at high speeds, were tested at a closed test site (Illinois Certification and Research Track, ICART), where a semitruck at varying speeds (30 to 70 mph) was driven to generate wind.

Table 2. Summarized Beaufort Wind Scale

Beaufort Number	Description	Wind Speed	Land Conditions
5	Fresh breeze	19–24 mph	Leaves of small trees begin to sway
6	Strong breeze	25–31 mph	Large branches in motion; whistling heard in telegraph wires; umbrellas used with difficulty
7	High wind, moderate gale, near gale	32–38 mph	Whole tree in motion; inconvenience felt when walking against the wind
8	Gale, fresh gale	39–46 mph	Twigs break off trees; generally impedes progress

Maximum wind gusts in Illinois vary by location and season. The last 20 years of weather records from the Illinois Climate Network (Illinois State Water Survey, n.d.) illustrate the expected maximum gust speeds (excluding outliers caused by tornadoes) averaged over years 2006–2025 per season in IDOT’s nine districts. Spring has the strongest average wind gusts, surpassing 35 mph statewide (8 on the Beaufort Scale). Summer and fall see the lowest average gust speeds, with no gusts larger than 30 mph statewide (6 on the Beaufort Scale).

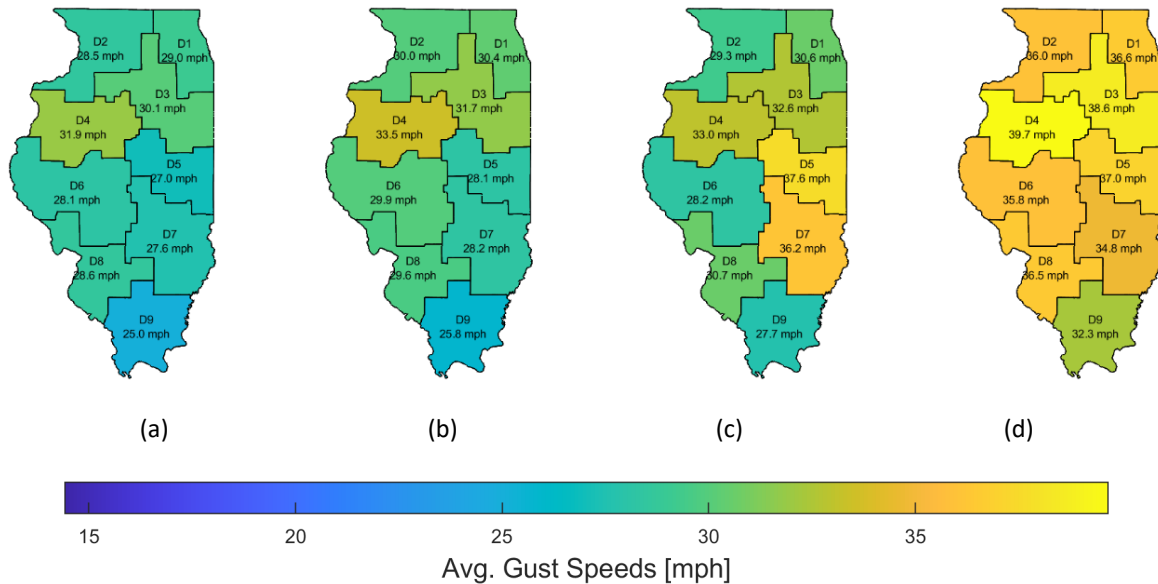


Figure 1. Illustration. Expected maximum gust speeds in Illinois by season: (a) summer, (b) fall, (c) winter, and (d) spring.

TRUCK-GENERATED WINDS

Truck-generated winds were evaluated in a controlled environment at IDOT’s ICART facility in Clinton County (southern Illinois), as illustrated in Figure 2. ICART furthers IDOT’s capabilities in characterizing pavement surface properties and identifying how those properties impact vehicles and passengers.



Figure 2. Photo. Aerial photograph of ICART.

Source: Adapted from Quigg Engineering Inc.

Field Experiment Setup and Data Collection

At ICART, IDOT provided a semitruck and trailer to replicate winds generated by a passing semitruck. The ICART track is more than 4,000 ft in length, which allows the provided semitruck to accelerate to 70 mph, maintain that speed through a 400 ft long section where the selected sign stands were placed, and safely slow down in the remaining 1,000 ft. The pavement widens at both ends of the track, allowing the semitruck to maneuver and return.

The 400 ft section selected for placing the temporary sign support systems allowed us to install four systems at a time (100 ft distance between sign stands). They were installed on the sides of the track (a mix of grass and gravel) following *MUTCD* guidelines. They were made level using sandbags (as foundation) and their leveling legs. Sandbags were also used as ballasts to secure the legs of all tested sign stands. The 48 in. diamond-shaped signs (provided by IDOT) were installed according to the specifications of each tested temporary sign support system (e.g., maximum sign height and distance to the track).

In all experiments, the semitruck traversed the closest lane to the tested sign support systems (see lane 3 in Figure 3-b). While isolated from traffic, ICART is open to natural winds. The experiments were carried out on a single day with low winds (August 12, 2025). To measure the speed of the wind generated by the passing semitruck, we placed wind speedometers near the bottom of the diamond-shaped sign, using the bottom bracket that supports the installed 48 in. sign. Table 3 presents the planned testing scenarios, including two sets of four temporary traffic stands. Set 1 was formed by two tall four-legged stands with springs, one tripod stand, and one short four-legged stand with springs. Set 2 was formed by one traffic sign stand from each group.

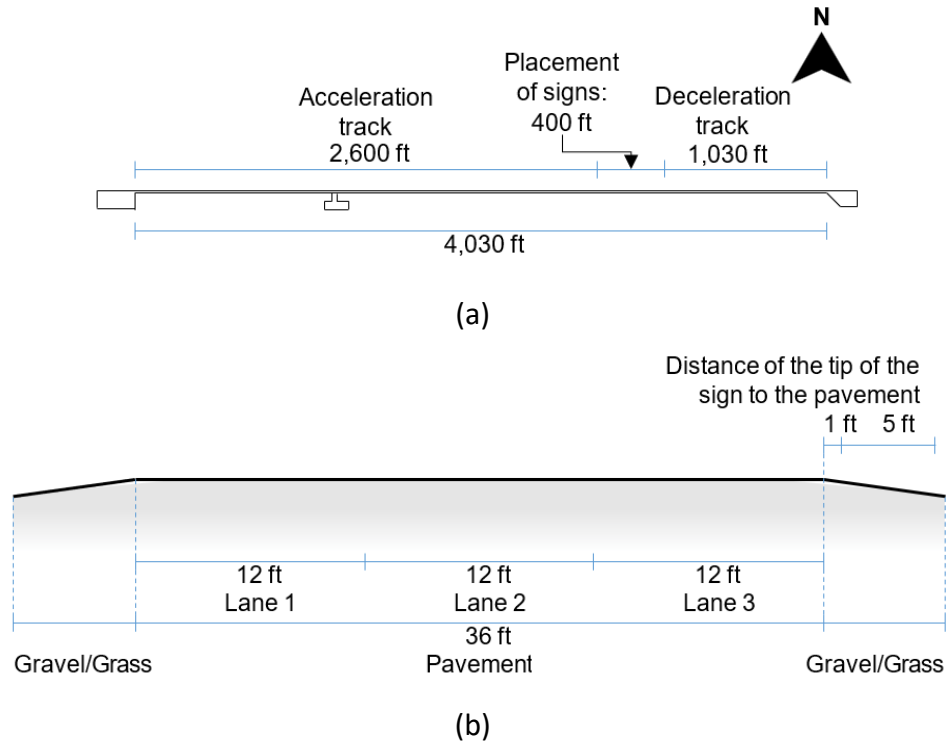


Figure 3. Schematic. ICART field experiments at (a) track separation, (b) cross-section of the track.

Table 3. Planned Experimental Scenarios

Test ID	Semitruck Speed	Sign Distance	Tested Stands	Note
1	30 mph	6 ft	Set 1	Executed
2	70 mph	6 ft	Set 1	Executed
3	70 mph	1 ft	Set 1	Executed
4	30 mph	1 ft	Set 1	Cancelled
5	30 mph	6 ft	Set 2	Cancelled
6	70 mph	6 ft	Set 2	Cancelled
7	30 mph	1 ft	Set 2	Cancelled
8	70 mph	1 ft	Set 2	Cancelled

The experiments were recorded using a fixed video camera, filming all four tested signs simultaneously, and photographed with smartphones. After each semitruck pass, we recorded the wind speed from the wind speedometer (which tracked the top wind speed of the last 5 minutes).

Data Analysis

Of the planned experimental scenarios, only the first three were performed, pictured in Figure 4. No measurable displacements or tip deflection of the signs were observed in the tests. The only observable results include slight wobbling of the tested tripod in Set 1.

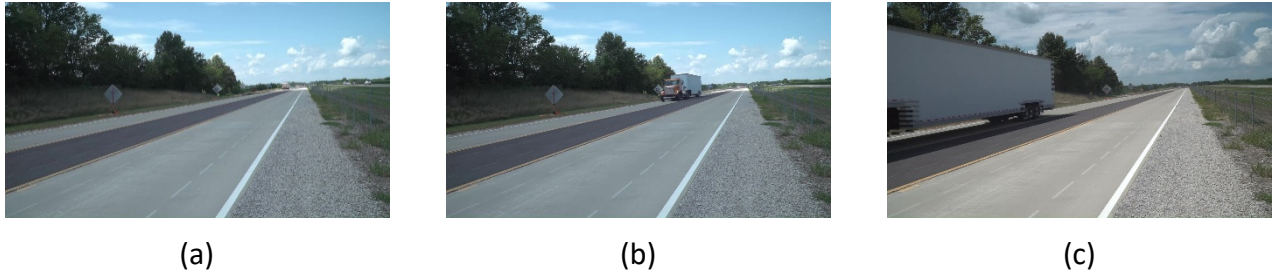


Figure 4. Photos. Selected frames from recorded videos of different tests: (a) beginning of test 1, (b) middle of test 2, and (c) end of test 3. Videos available at: [ICART experiment videos](#).

During Tests 1 and 2, the wind speedometers did not record significant winds from either the truck or nature. The wind speedometers recorded maximum winds between 11 and 13 mph during Test 3. Also, the wind speedometers did not have consistent measurements, which varied depending on the angle and placement. Tests 4 to 8 were cancelled because none of the first tests presented any measurable displacements and, at most, a moderate breeze (4 on the Beaufort Scale).

FAN-GENERATED WINDS

It remains challenging to predict exactly when a windy day will occur. Therefore, we organized efforts to simulate, in a semi-closed environment, wind gusts using industrial fans inside Illinois Center for Transportation (ICT) facilities.

Experiment Setup and Data Collection

The experimental setup involved installing a group of fans that will generate wind loads at several angles. The fans were installed at a height that maximizes the surface of a sign facing the generated winds. Therefore, as illustrated in Figure 5, fans were lifted from the ground depending on the height of the traffic sign stand being tested.

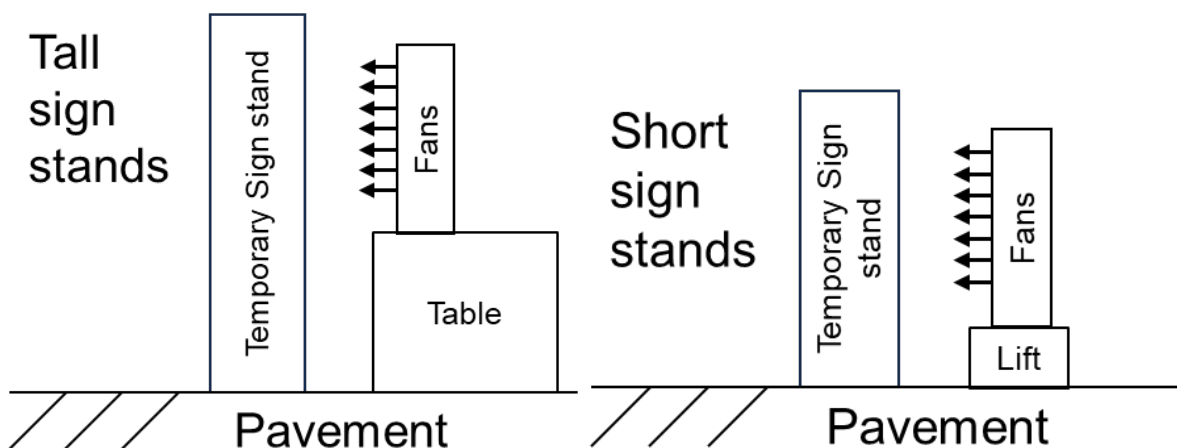
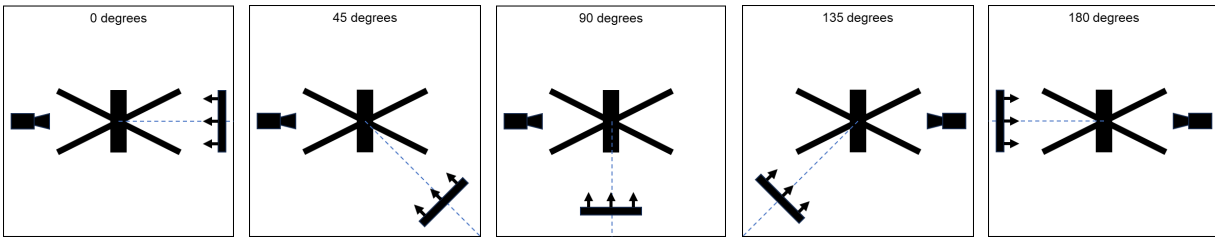


Figure 5. Diagram. Position of the installed fans depending on the height of the tested sign support system.

The experiments were recorded in three-minute videos used to measure tip deflections and displacements. Figure 6 shows the position of the camera and the fans relative to the traffic sign stands for each tested wind direction. Note that the camera is always positioned facing the sign or its back. (A lateral view cannot capture side-to-side sway and other displacements.) To ensure the fans were working properly before recording, wind speed at the bottom of the 48 in. diamond-shaped signs was measured with the same wind speedometers used to measure the truck-generated winds. Since the concrete floor of the ICT facility is level, the tests did not use sandbags to level signs or as ballasts to secure sign support systems in position.



Only on those that are not symmetrical.

Figure 6. Diagrams. Positioning of the recording camera and fans relative to the tested temporary sign support system.

Data Analysis

Out of all selected temporary sign support systems, only two were tested in all positions. (Both are shown in Figure 7.) The recorded wind speeds for the experiments were 14 mph, near the maximum wind speed generated by the fans of 17 mph (estimated based on their diameters and maximum air flow). This indicates that even at considerable proximity (1 ft or 2 ft distance), there is considerable loss of power due to spread. The tested signs did not present displacement in relation to their initial ground position or side-to-side sway, so tests on other traffic sign stands were cancelled.



Figure 7. Photos. Experimental setup using fans to generate artificial winds: (left) tall four-legged sign support system with springs, and (right) tripod sign support system.

NATURAL WINDS

The windy season in Illinois starts in late October. We identified days of strong winds, with gusts above 30 mph, at ICT (Rantoul, Illinois) and placed the selected sign support systems in open space.

Experiment Setup and Data Collection

We used wind direction from the weather forecast to position 8 of the 12 selected sign support systems so that their signs face the wind and have minimal interference from nearby buildings. The initial position of each sign support system was marked on the ground. A camera was used to record the deflections and displacements of the tested sign support stands. The camera was positioned far from the tested stands to capture all tested sign support systems simultaneously, as illustrated in Figure 8, without interfering with the winds hitting the sign stands.



Figure 8. Illustration. Position of recording camera and tested traffic sign stands.

Three one-hour experiments were recorded. In the first one, sign support systems were placed directly over the pavement without using sandbags (for leveling or securing position). If a sign support system failed during the first experiment, it was positioned back in place until the end of the test period. Any support system that failed at least once during an experiment was secured in place with ballasts for the next experiment. If by the end of the test period a support system stand did not fail, but was displaced from its starting position, the distance and direction of the displacement was measured and recorded. The sign support systems that did not fail or experience any displacements were replaced by the remaining temporary sign support systems.

Data Analysis

The first days that met the gust speed criterion were October 21 and 22, 2025. On the first day (October 21), the winds peaked between 11 a.m. and 3 p.m. with wind speeds of 20–30 mph and a peak gust of 34 mph (based on the weather forecast at weather.com). On the second day (October 22), the winds were slightly weaker with speeds of 15–25 mph and peak gusts of 31 mph, peaking between 9 a.m. and 12 p.m. Two of the one-hour experiments were recorded during the first day, and the third experiment was recorded during the second day.

Throughout the first experiment, two signs failed multiple times. One system in the tripod group failed in a few seconds whenever winds were 20 mph. One system in the short four-legged group without springs failed twice. On the other hand, one system in the tall four-legged group with springs was the only system that suffered some displacement from its initial position (< 2 in. total) in the same direction as the wind (WNW). Other systems neither failed nor had measurable displacement.

For the second experiment, both failing systems (from the tripod group and short four-legged without springs group) received ballasts and were positioned back in place. Of the five systems that

neither failed nor had measurable displacements in the first experiment, we replaced four (chosen randomly) to include the remaining four selected systems in the second experiment. Systems that received ballasts were kept in the second and third experiments. No additional displacements were measured and no systems failed in the second and third experiments. Nonetheless, in all experiments, spring-based systems (both tall and short four-legged spring-based systems) presented significant tip deflection, responding to the wind without suffering displacements or failing.

PROFILING OF WIND GUSTS AND SIGN TIP DEFLECTION

Despite being informative, previous experiments were unable to evaluate the exact response of the selected temporary sign support systems to wind gusts. To that end, the last set of field experiments involved associating the tip deflection of selected sign support systems with the gusts hitting their signs in real time.

Experiment Setup and Data Collection

Two systems from the short four-legged with springs group (SW-484-25 and MDI 50SM-2S) were separated to evaluate tip deflections against gusts. We did not test non-spring-based systems, because they were not designed to have deflection as a response to transient winds. As illustrated in Figure 9, a camera and two speedometers were placed to the side of the tested system. The system and wind speedometers were both positioned facing the wind.



Figure 9. Photo. Experimental setup to measure the profile of the wind causing deflections to a spring-based sign support system.

Each experiment lasted 10 minutes. During this period, the camera recorded the system's deflection while we recorded the maximum wind speed measured by the speedometers in the past 15 seconds. These readings were stored in an MS Excel spreadsheet. A total of six experiments were performed, three for each selected sign support system.

Data Analysis

The experiments were carried out on November 11, 2025, a day with 20–30 mph SSW winds, gusts of 34 mph, and no recorded precipitation. Experiments were conducted between 11 a.m. and 2 p.m., periods with the strongest winds, according to the weather forecast (weather.com). It is important to note that in an interval of 15 seconds, the wind speeds vary significantly and cannot be treated as uniform. Figure 10 shows the measurements of all experiments. Note that the first experiment with MDI 50SM-2S stopped midway because the speedometers could not obtain readings due to a short period with no winds (maximum of 4 mph), so the data were discarded. At the end of the third experiment with MDI 50SM-2S, the winds started to slow down, and no further experiments were conducted.

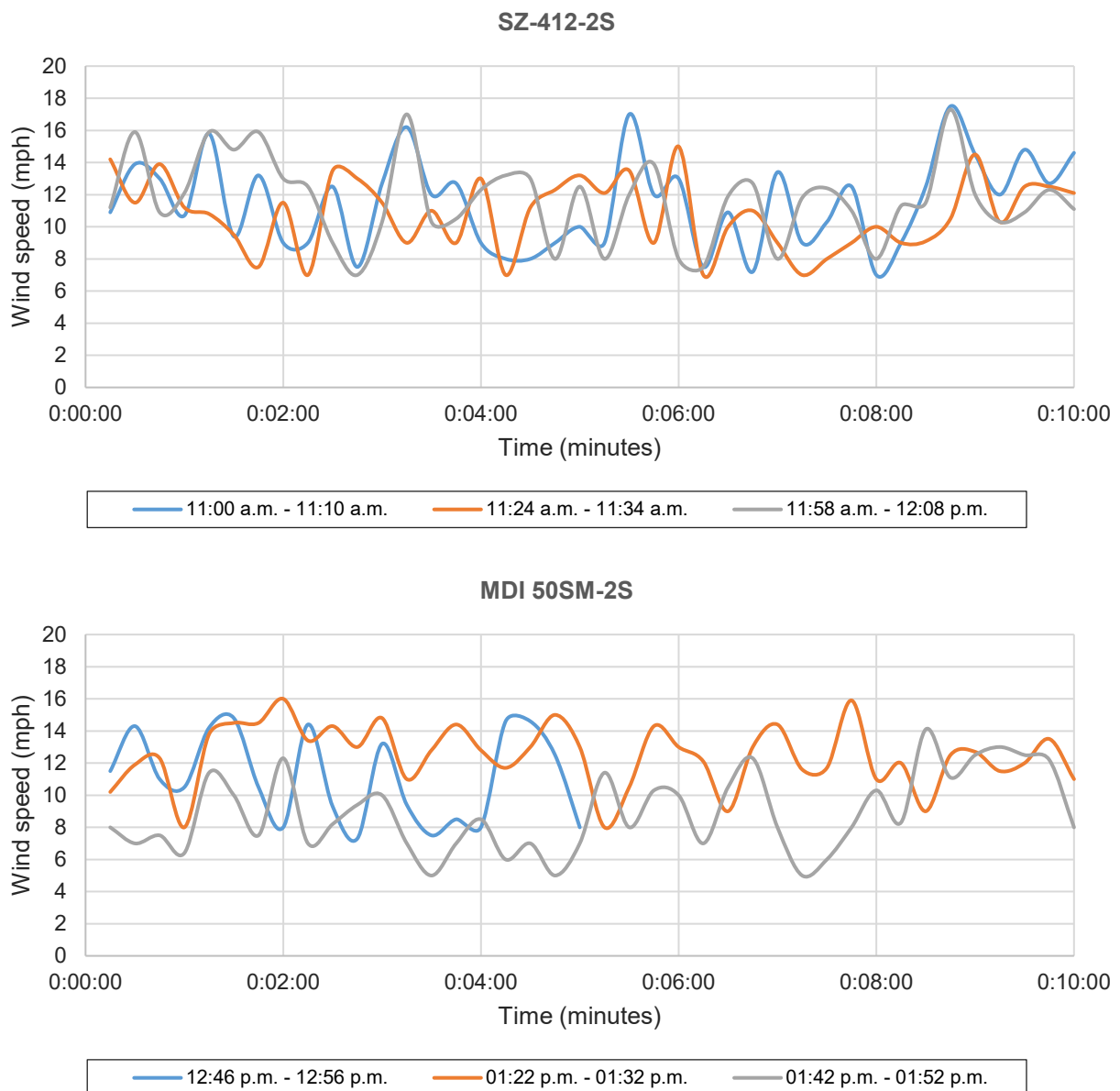


Figure 10. Graph. Recorded wind speeds during experiments with two sign stands.

It is important to note that the measured wind speeds are significantly lower than the weather forecast because the wind speedometers had to be placed near the ground, creating interference. However, the measured wind patterns were consistent with the tip deflections, where periods with higher winds were reflected in both the measured wind speeds and the observed tip deflections. Nonetheless, it is imperative to point out the challenges in measuring natural wind speeds in real time, where the wind speedometers were unable to capture fast-changing wind speeds because of an internal delay processing the speed in which its fan was rotating. Therefore, if a gust hits the speedometer's fan and slows down before the speedometer's fan could rotate at the right speed, the speedometer will record a lower wind speed than that of the gust.

CHAPTER 4: FINITE-ELEMENT ANALYSIS OF WIND-INDUCED STRUCTURAL RESPONSE OF TEMPORARY SIGN SUPPORT SYSTEMS

Field observations and past incidents in Illinois and other states suggest that temporary traffic signs can be damaged, displaced, overturned, or intermittently unreadable when exposed to moderate natural winds and vehicle-generated gusts—especially in flat, wind-prone environments. These effects are often intensified when large vehicles pass nearby, creating brief but strong aerodynamic disturbances around the sign assembly. In particular, heavy trucks traveling at highway speeds can generate short-duration gusts that impose high-magnitude aerodynamic loads on nearby signs. While these transient forces may not trigger immediate structural failure, they can still cause noticeable oscillations, rotations, and large deflections that reduce sign visibility and message clarity. From an operational safety perspective, the key concern is that excessive motion can reduce driver comprehension time and lead to missed or misinterpreted messages. Spring-based sign stands, for example, often resist overturning but can undergo substantial swinging during gust events, highlighting a trade-off between structural stability and message readability. This motivates a modeling approach that can resolve transient aerodynamic pressures and deterministically quantify the resulting displacements for serviceability and readability limits. Therefore, to investigate these behaviors, numerical modeling was conducted using computational fluid dynamics (CFD) and finite-element analysis (FEA).

METHODOLOGY

A sequential CFD-FEA workflow was developed to simulate transient aerodynamic loading on temporary traffic signs and to compute their structural response under natural gusty winds and heavy vehicle-induced wind effects (e.g., truck pass-by disturbances). The overall modeling framework is summarized in Figure 11 and was implemented using Autodesk Fusion 360, ANSYS Fluent, and ANSYS Mechanical 2025 within the ANSYS Workbench environment.

First, manufacturer specifications and measured dimensions were used to develop a detailed 3D geometric representation of the temporary sign system in Autodesk Fusion 360. Based on this geometry, a computational fluid domain and associated boundary conditions were defined in ANSYS Fluent 2025 following best practice recommendations from the literature (Franke et al., 2007). The fluid mesh was then generated and refined to discretize the domain, with localized refinement near the sign panel, support members, and ground surface, along with near-wall inflation layers to resolve boundary-layer behavior and unsteady flow separation. An unstructured hybrid Poly-Hexcore mesh (polyhedral cells with hexahedral core regions) was generated in ANSYS Fluent Meshing to resolve near-field aerodynamic effects while maintaining computational efficiency in the far field. Dynamic meshing (fluid mesh is allowed to move or deform during the simulation) was enabled so the fluid mesh could deform automatically in response to structure-induced motion at each time step.

Following mesh generation, transient CFD simulations were performed to resolve the time-dependent airflow around the sign assembly and capture unsteady aerodynamic phenomena,

including vortex shedding, wake development, and spatially varying surface-pressure fluctuations. The resulting surface pressure and nodal forces were extracted at each time step and transferred to ANSYS Mechanical through the Workbench System Coupling tool, enabling a two-way fluid-structure interaction (FSI) analysis.

In parallel, the same geometry was set up in ANSYS Mechanical by defining material properties, connections, and support conditions, followed by generation of the structural mesh. At each coupled step, aerodynamic loads from Fluent were mapped onto the structural surfaces, and transient structural analyses were conducted to evaluate wind-induced deflections, deformation patterns, vibration response, sign-tip displacement, and equivalent stress under the prescribed wind conditions. The computed structural displacements were then returned to System Coupling and passed back to Fluent to update the dynamic mesh. This feedback cycle repeated sequentially until the final simulation time was reached.

At the end of the analysis, ANSYS Mechanical provided the full time history of the structural response (e.g., tip displacement), enabling us to estimate total deformation under the prescribed wind speeds. We then converted the displacement response to the corresponding sign tilting angle, which is more intuitive for users, and compared it with commonly used serviceability-based performance estimates derived from sign legibility. Repeating this workflow across multiple sign configurations enables an efficient and consistent comparative assessment.

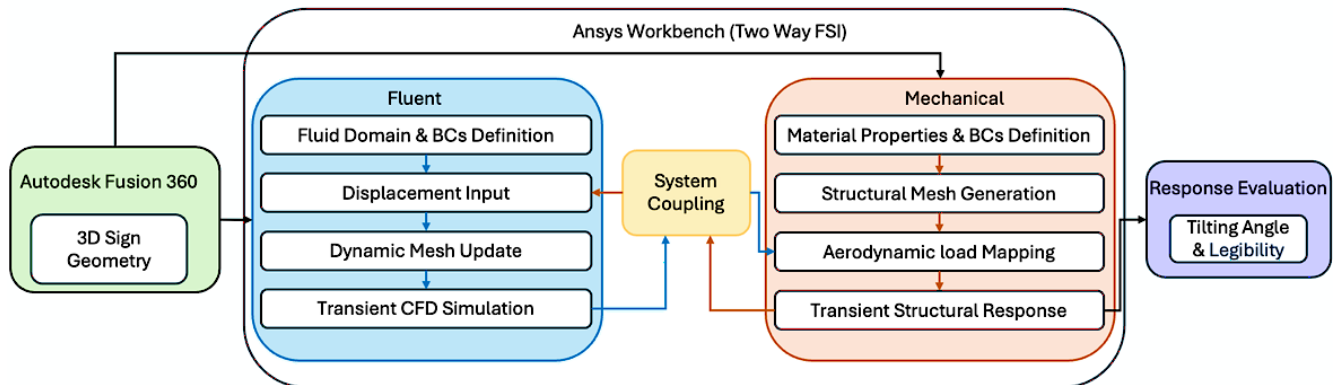


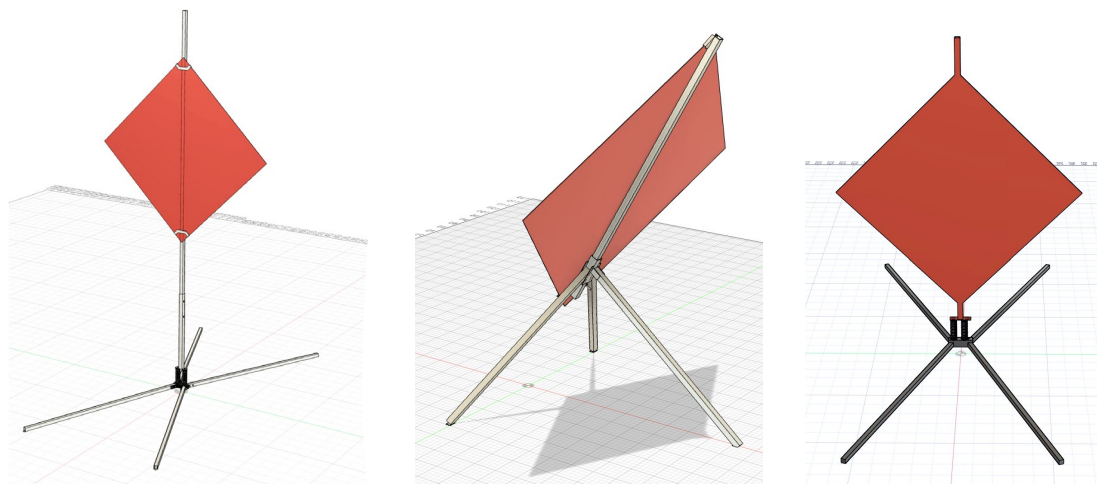
Figure 11. Diagram. Flowchart of the numerical modeling framework.

3D Sign Stand Geometry Preparation

Despite the limited availability of detailed manufacturer-specific structural data for temporary traffic sign systems, simplified yet physically sound representative 3D models were developed to reduce computational cost and limit numerical uncertainty associated with complex geometries. These models capture the essential geometric, mechanical, and load-transfer characteristics observed in field-deployed temporary sign stands. The complete 3D geometry for all sign-stand configurations was prepared using Autodesk Fusion 360.

The baseline configuration corresponds to the 4860M temporary sign stand equipped with a 48 × 48 in. aluminum sign panel manufactured by MDI Worldwide. This configuration represents a widely used four-legged sign stand incorporating a spring-based base assembly and was adopted as the primary reference model for finite-element analysis. The modeled system consists of a steel base plate connected to four outward-spreading aluminum legs, with two coil springs included to represent yielding behavior and flexibility under wind-induced loading. The legs were modeled using 1.25 × 1.25 in. square hollow aluminum sections, forming an open footprint of approximately 55 × 122 in. to enhance global stability. The vertical support was represented as a two-stage telescoping upright composed of nested square aluminum tubes with cross-sectional dimensions of 1.5 in. and 1.25 in. and a wall thickness of 0.10 in. (2.54 mm). An adjustable mounting height was incorporated, and a designated breakaway section located approximately 19 in. (483 mm) above grade was included geometrically; however, fracture or separation behavior was not explicitly modeled. The sign panel was modeled as a diamond-shaped aluminum plate measuring 48 × 48 in. with a thickness of 0.080 in. and was attached to the upright using simplified bracket connections. The modeled geometry reflects the as-tested field configuration, with a mounting height of 5 ft measured from grade to the lower corner of the sign and an overall stand height of approximately 132 in., excluding sign flags. The total device weight in the field configuration was approximately 53.0 lb. During field testing, additional stability was provided by 25.0 lb. sandbags placed on each leg. The stabilizing effect of this ballast was represented through boundary condition adjustments rather than explicit contact modeling.

In addition to the baseline configuration, two alternative sign stand geometries, the WZ-448 Apex Tripod manufactured by Eastern Metal of Elmira Inc. and the 50SM-2S Sign Stand manufactured by MDI Worldwide, were modeled to represent differences in sign plate height, overall stability, base assembly, and load-transfer mechanisms. These configurations were included to enable a comparative evaluation of wind-induced tilting angles under similar aerodynamic loading conditions. Structural models for all configurations are shown in Figure 12.



(a) 4860M (MDI Worldwide)

(b) WZ-448 Apex Tripod (EM)

(c) 50SM-2S (MDI Worldwide)

Figure 12. Illustration. Structural models of temporary sign stands with different configurations in Autodesk Fusion 360.

Computational Domain Definition

To simulate wind loading and evaluate the resulting surface pressure and aerodynamic forces acting on the sign plate, each sign stand model was embedded within a 3D computational fluid domain, as illustrated in Figure 13. The computational domain was defined as a bounded region, $\Sigma \subset \mathbb{R}^3$ surrounding the sign panel and its supporting structure at their initial position. This domain provides sufficient spatial extent to capture upstream flow development, near-field pressure distributions, and downstream wake evolution associated with wind-structure interaction. The boundary of the computational domain is expressed as

$$\partial\Sigma = \Gamma_{in} \cup \Gamma_{out} \cup \Gamma_{side} \cup \Gamma_{top} \cup \Gamma_{gnd},$$

where Γ_{in} and Γ_{out} denote the inlet and outlet boundaries, respectively; Γ_{side} represents the lateral boundaries; Γ_{top} corresponds to the upper boundary; and Γ_{gnd} defines the ground surface. Following established best practice guidelines for external-flow CFD simulations and wake-resolving domain design reported in the literature (Franke et al., 2007), the domain dimensions were selected to minimize blockage effects and artificial boundary interference. Specifically, the inlet length was set to satisfy $L(\Gamma_{in}) \geq 5D$, while the outlet length was extended to $L(\Gamma_{out}) \geq 15D$, where D is the characteristic length of the sign plate edge. Lateral and vertical clearances on the order of $5D$ were also provided to allow unconfined flow development and proper wake expansion.

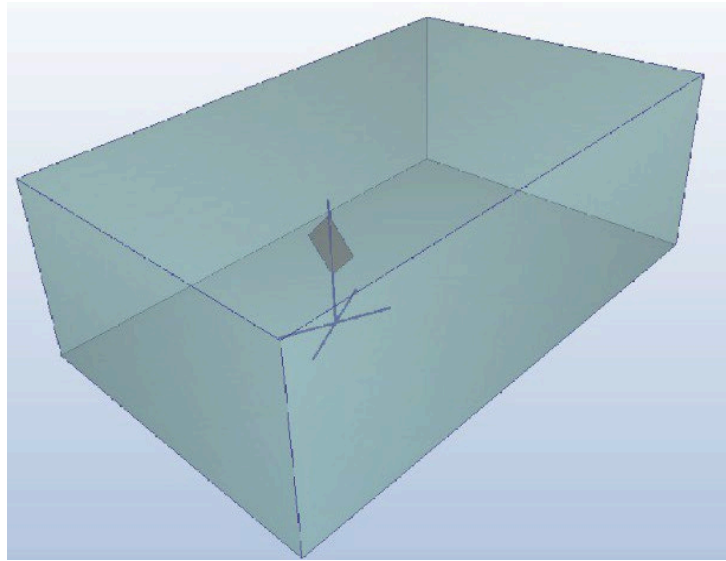


Figure 13. Illustration. Computational fluid domain used for the fluid flow simulation in ANSYS Fluent 2025.

Boundary conditions were assigned based on the physical characteristics of the problem. The ground boundary Γ_{gnd} was modeled as a no-slip wall to represent surface roughness effects and near-ground shear. The inlet boundary Γ_{in} was prescribed as a velocity inlet with a specified wind profile, while the outlet boundary Γ_{out} was treated as a pressure outlet. The lateral and top boundaries were modeled using far-field or symmetrical conditions, as appropriate, to approximate open-flow behavior and reduce artificial reflections. This domain and boundary condition configuration provides adequate

spatial clearance to resolve upstream flow behavior, near-field pressure gradients on the sign surface, and downstream wake dynamics. The resulting time-dependent aerodynamic pressure and force fields extracted from the CFD simulations serve as direct inputs for subsequent CFD-FEA load transfer and structural deformation analyses.

Material Properties and Model Assumptions

Material properties were assigned using representative values corresponding to commercially available temporary traffic sign components. All aluminum members, including the legs, telescoping upright, and sign panel, were modeled as linear-elastic, isotropic Aluminum Alloy 6061-T6, with standard elastic modulus, Poisson’s ratio, and mass density. Steel components, including the structural connectors, were modeled as linear-elastic structural steel.

Several modeling assumptions and idealizations were introduced due to the computational expense of the study. Figure 14 illustrates the replacement of the spring assembly geometry with an equivalent structural bushing joint representation. This idealized model was calibrated to reproduce the mechanical behavior of the original spring coil, capturing its global stiffness and load-deformation response while significantly reducing structural complexity.



Figure 14. Photo and Illustration. Equivalent structural idealization of spring assemblies for finite-element modeling: (left) photo from field experiment; (right) model in ANSYS Mechanical 2025.

Mechanical joints (e.g., bolts, nuts, and brackets) were idealized as rigid connections based on their functional role, without explicitly modeling individual fasteners. As shown in Figure 15, ground-structure interaction effects, such as surface friction, soil compliance, and uneven terrain, were not explicitly represented. Instead, a fixed-base boundary condition was applied to represent a properly secured, ballasted installation, consistent with field observations that four-legged sign stands did not dislocate when sandbag ballast was used. These modeling assumptions were intentionally conservative with respect to overall stability and were selected to emphasize the primary aerodynamic load transfer mechanisms and global structural response, rather than installation variability or localized component-level failure.

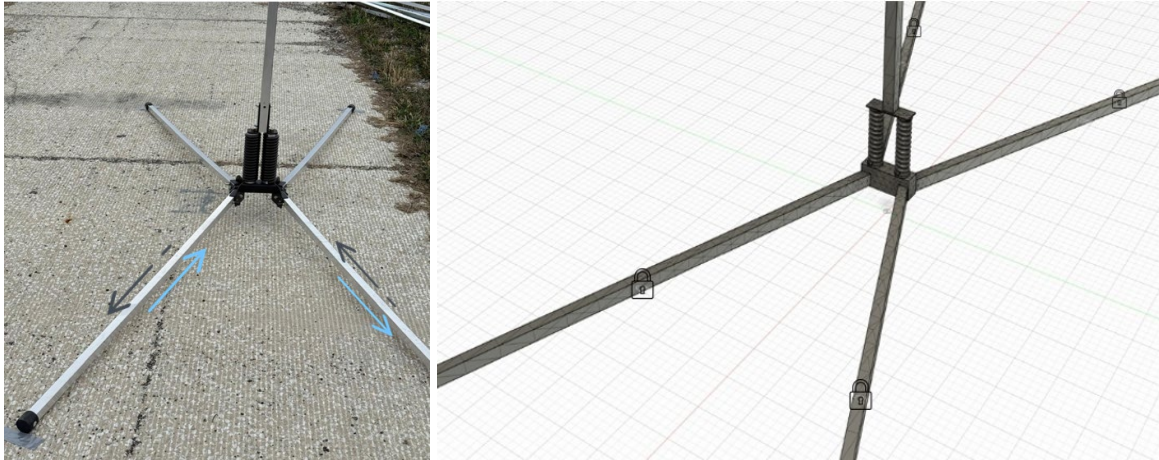


Figure 15. Photo and Illustration. Idealized fixed-base boundary conditions represent secured and ballasted conditions: (left) photo from field experiment; (right) model in Autodesk Fusion 360.

Transient Wind Simulation

In this study, we build models to generate two types of transient wind: natural gusty wind and wind induced by passing heavy vehicles (e.g., trucks).

Natural Gusty Wind

To represent gust-like wind conditions, synthetic, time-varying inlet velocity profiles were applied at the domain inlet. These profiles were derived from the field experiments, with representative peak wind speeds defined using long-term meteorological observations from Illinois. Specifically, peak values were selected based on approximately 20 years of wind records from Illinois Climate Network, as summarized in Figure 16 (Illinois State Water Survey, n.d.).

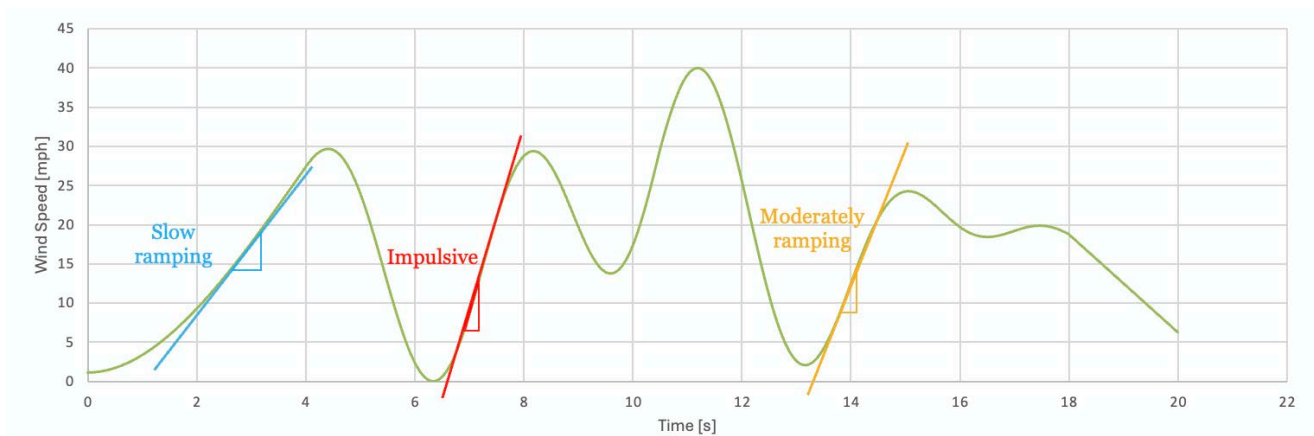
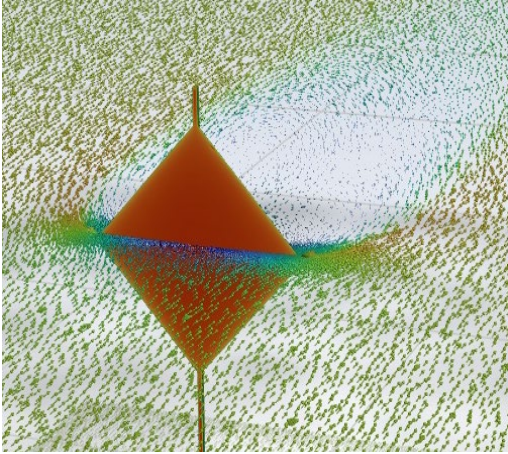


Figure 16. Graph. Synthetic gust profiles used for transient CFD inlet conditions.

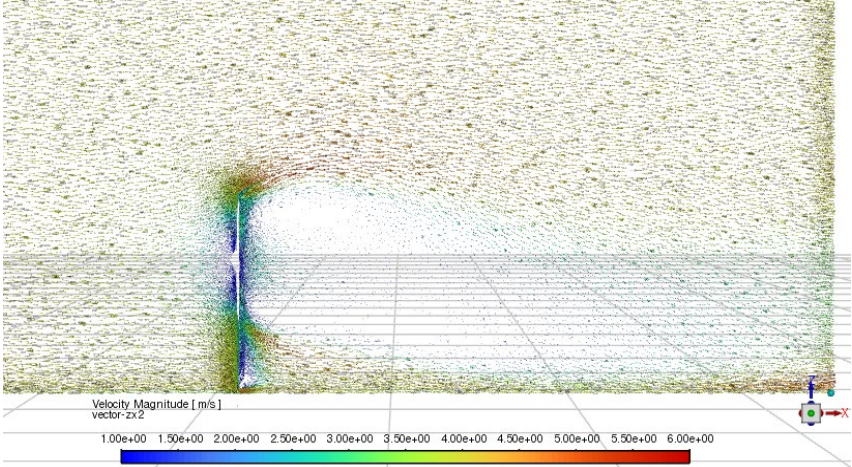
These transient inlet conditions were applied at the fluid-domain inlet, enabling simulation of short-duration velocity peaks and rapid flow variations that are not captured by steady (static) CFD approaches. The incompressible Reynolds-averaged Navier-Stokes equations were solved using the

shear-stress transport $k-\omega$ turbulence model, which is well suited for flows with separation, adverse pressure gradients, and near-wall effects. This approach provides a practical balance between numerical robustness and the ability to capture dominant unsteady flow structures relevant to wind-structure interaction (Ansys Fluent User's Guide, 2025).

Temporary traffic signs behave aerodynamically as bluff bodies, and their sharp edges promote flow separation and unsteady wake formation. Prior work shows that, at low wind speeds, vortex shedding from the cantilever arm can cause large-amplitude vibrations across multiple wind directions, whereas at high wind speeds, buffeting produces smaller-amplitude vibrations (Zuo & Letchford, 2010). These unsteady mechanisms can result in time-dependent pressure fluctuations on the sign surface. Representative flow features, including near-edge separation, wake development, and downstream vortex structures, are illustrated in Figure 17, which presents transient CFD visualizations of the flow field around the temporary sign.



(a)



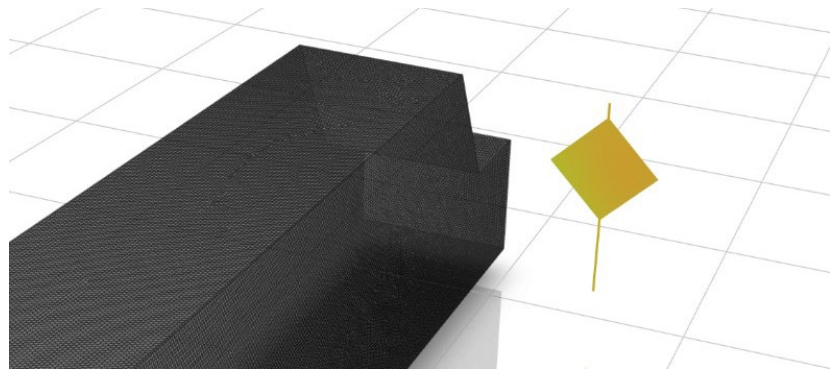
(b)

Figure 17. Illustrations. Transient CFD visualizations of the flow field around the temporary sign support system in ANSYS Fluent 2025: (a) near-edge flow separation and vortex formation, and (b) downstream wake development in the sign's lee region.

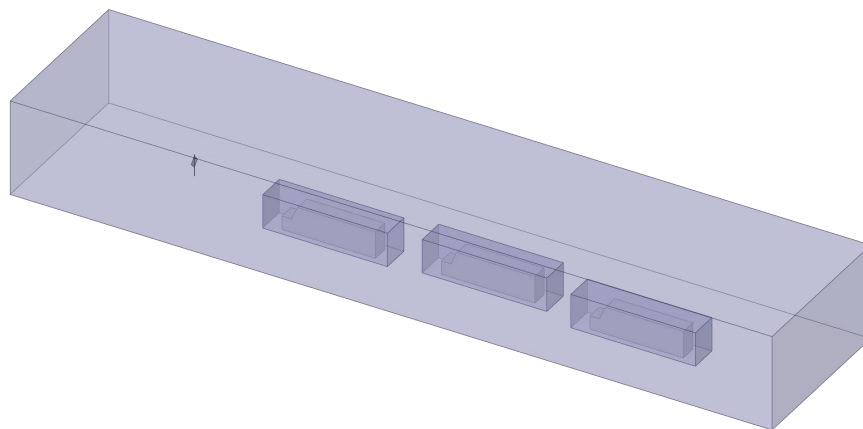
Truck-Induced Wind

We also considered heavy vehicle–induced loading by simulating a truck passing at high speed near the temporary sign. The primary scenario involved a single heavy truck traveling at 70 mph, as illustrated in Figure 18-a. The sign was positioned near one side of the domain to represent roadside placement consistent with *MUTCD* lateral-offset guidance (e.g., a 6 ft minimum offset from the edge of the shoulder, where applicable) (FHWA, 2023). The truck motion was prescribed using a time-dependent translational velocity with a smooth ramp-up at the beginning, while the sign remained stationary. To isolate vehicle-induced aerodynamic effects, no ambient wind was imposed (i.e., the inlet velocity was set to zero). Time-resolved pressure histories extracted from the sign surface were subsequently used as direct inputs for the structural response analysis.

In addition, a multi-truck platoon case involving three trucks was simulated to evaluate cumulative effects (Figure 18-b). In this configuration, the trucks were aligned in a streamwise direction with clearance of 300 ft, and no ambient wind was applied. While this clearance is smaller than the full AASHTO stopping sight distance at similar highway speeds (which may exceed 600–800 ft) (Harwood et al., 1989), it represents a more severe loading configuration for evaluating tip displacement under sequential wake interactions.



(a)



(b)

Figure 18. Illustrations. Heavy vehicle–induced aerodynamic gust simulations in ANSYS Fluent 2025: (a) single-truck pass-by scenario, and (b) three-truck platoon configuration.

However, real-world conditions would involve the combined influence of vehicle-induced gusts and ambient wind, potentially amplifying sign deflections and oscillations. Therefore, compounded wind scenarios involving both truck-induced and natural winds are identified as a promising future research topic.

Meshing Strategy

In finite-element analysis, a mesh is a network of small, simple geometric shapes (called elements) used to represent the overall geometry of a physical object. Because computers cannot solve the governing equations for an entire object in a single step, meshing allows the solver to compute the response element by element and then stitch those results to predict the behavior of the full structure. In general, a finer mesh provides higher accuracy but increases the number of elements and, therefore, computational cost. In this study, both the structural and fluid domains were discretized using 3D meshes tailored to the requirements of FEA and CFD. The meshing strategy was designed to resolve deformation, stress transfer, and unsteady flow features near the sign structure while maintaining computational efficiency in the far field.

Fluid Meshing

The computational fluid domain was discretized using an unstructured hybrid Poly-Hexcore mesh (polyhedral cells near the geometry and a hexahedral core in the far field), as illustrated in Figure 19. Near-wall inflation layers were applied along the sign panel, upright, legs, and ground surface to resolve boundary-layer behavior and near-wall velocity gradients. Inflation was implemented using wedge elements with a smooth transition, a maximum of five layers, and a growth rate of 1.2. Mesh refinement was concentrated near the sign structure and in the near-wake region to capture flow separation, strong pressure gradients, and unsteady wake development. Away from the sign, a progressively coarser mesh was used to reduce computational cost while preserving overall flow accuracy.

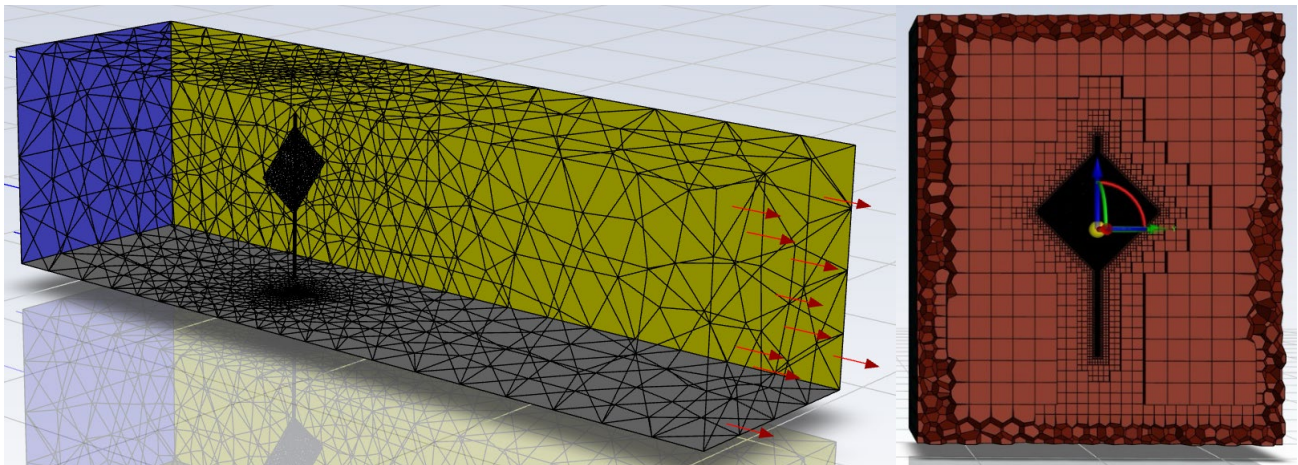


Figure 19. Illustration. Unstructured hybrid Poly-Hexcore CFD mesh. (Left) Isometric view of the full fluid domain. (Right) Y-Z cross-sectional plane near the sign structure in ANSYS Mechanical 2025.

CFD mesh quality was evaluated using standard metrics. The minimum orthogonal quality was 0.225, and the maximum aspect ratio was 152.4; both occurred in localized regions away from the primary load-transfer surfaces. These values fall within acceptable ranges for unsteady external-flow simulations involving complex bluff-body geometries (Ansys Fluent User's Guide, 2025). Overall, this meshing approach supported stable solver convergence and reliable prediction of time-dependent aerodynamic pressure and shear forces acting on the sign surfaces. An example of the CFD mesh distribution is shown in Figure 19, highlighting localized refinement near the sign structure, ground surface, and near-wake region.

Dynamic meshing is a CFD technique in which the computational mesh updates as geometry or boundaries move and/or deform over time. This allows the solver to capture prescribed motion, moving components, and fluid-structure interaction (FSI) without remeshing the entire domain at every time step. In the transient System Coupling simulations, the temporary sign displaced at each time step under wind loading; therefore, dynamic meshing (local remeshing) was enabled in the fluid domain around the sign to maintain mesh quality near the moving boundaries and to accurately capture the evolving pressure distribution. Figure 20 illustrates this process by showing how the mesh adapts and redistributes around a moving/rotating body to preserve element quality near the surface.

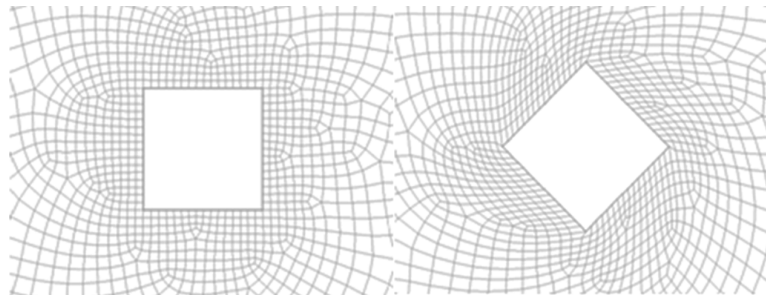


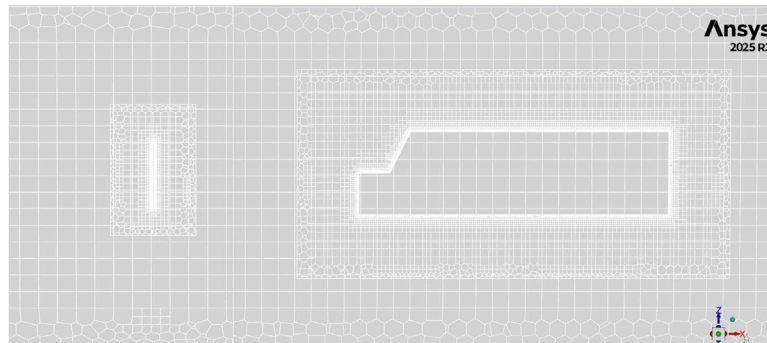
Figure 20. Illustration. Mesh deformation patterns around a moving body.

Source: Ansys Fluent User's Guide (2025)

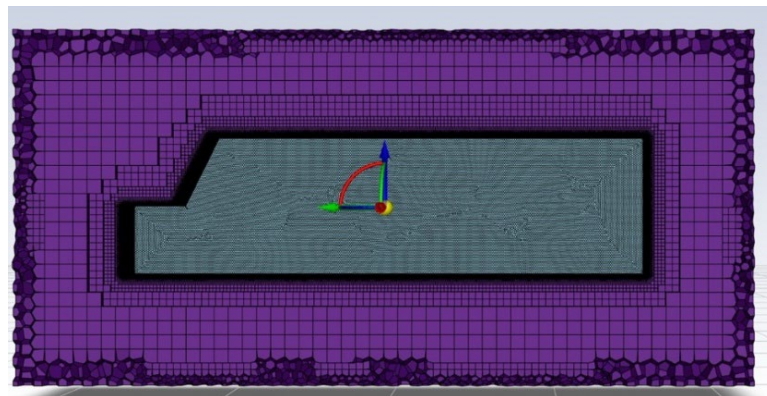
When a body undergoes large translation and rotation in a fluid domain, dynamic remeshing can become inefficient and may degrade mesh quality. To avoid this, we used an overset mesh approach, where each object is meshed separately and overlaps a stationary background mesh. Solution variables are transferred across the overlap via donor-to-receptor interpolation, allowing moving geometries to be simulated without remeshing the full domain and while maintaining local resolution near the object surfaces.

Accordingly, truck-induced aerodynamic loading was simulated in ANSYS Fluent 2025 using a truck-sign overset configuration (Figure 21). The roadway airflow was represented by a stationary background domain, while each truck was assigned to a moving overset region and the sign was assigned a stationary overset region. This setup enables stable vehicle motion, preserves wake development, and captures time-dependent pressure effects on the sign. The computational enclosure was elongated to provide adequate upstream development and downstream recovery length, minimizing boundary-induced artifacts.

The background-domain extents were selected using a characteristic length D , defined here as the representative truck height used to scale computational clearances in the streamwise and lateral directions. Using this definition, the enclosure provided at least $\geq 5D$ upstream clearance, $\geq 10D$ downstream clearance, and sufficient lateral clearance to reduce blockage effects (Franke et al., 2007). Local mesh refinement was applied around the truck surfaces, the sign panel, and the near-wake region to capture sharp pressure gradients and unsteady flow structures. Mesh resolution was considered adequate based on a sensitivity check, where additional localized refinement did not produce noticeable changes in the key flow features and pressure distributions relevant to load transfer.



(a)



(b)

Figure 21. Illustration. Overset mesh configuration in ANSYS Fluent 2025: (a) schematic of the background air domain with an overlapping stationary sign region and a moving truck region; (b) fluid mesh distribution around the truck surfaces.

Structural Meshing

In parallel, the structural components were discretized using 3D solid finite elements suitable for thin-walled tubular members and plate-like parts. A tetrahedral solid-element formulation was chosen to capture global deformation and dynamic response under transient wind loading. Local mesh refinement was applied in regions expected to exhibit high stress gradients or large deformation, including the base-to-upright connection, the telescoping joint, the sign mounting brackets, and the spring attachment zones. The final structural mesh contained adequate resolution

for deformation and performance assessment while maintaining numerical stability. Mesh adequacy was confirmed through a qualitative sensitivity check, in which additional local refinement produced no noticeable changes in global deformation patterns or monitored displacement, and the minimum element quality remained above 0.15 (Ansys Fluent User’s Guide, 2025). The structural finite-element mesh and the corresponding element quality distribution are shown in Figure 22.

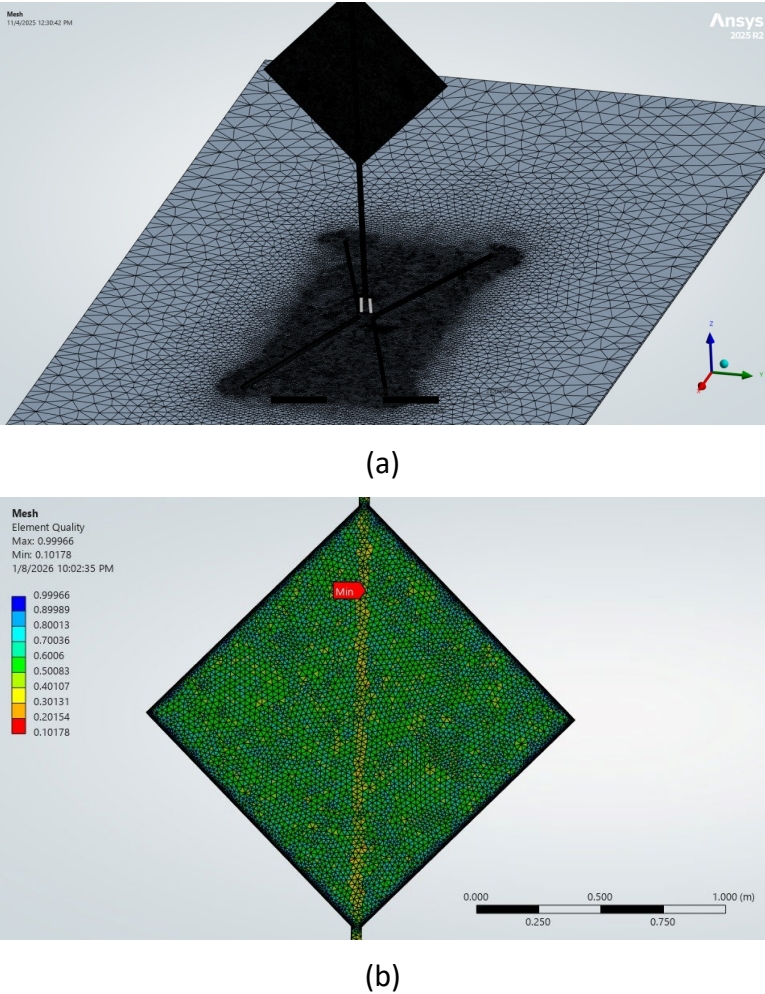
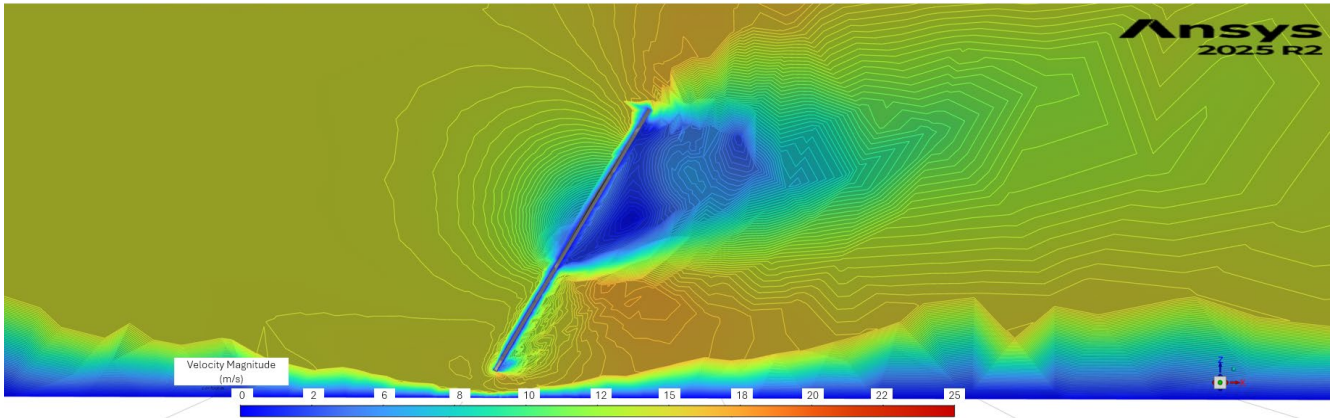


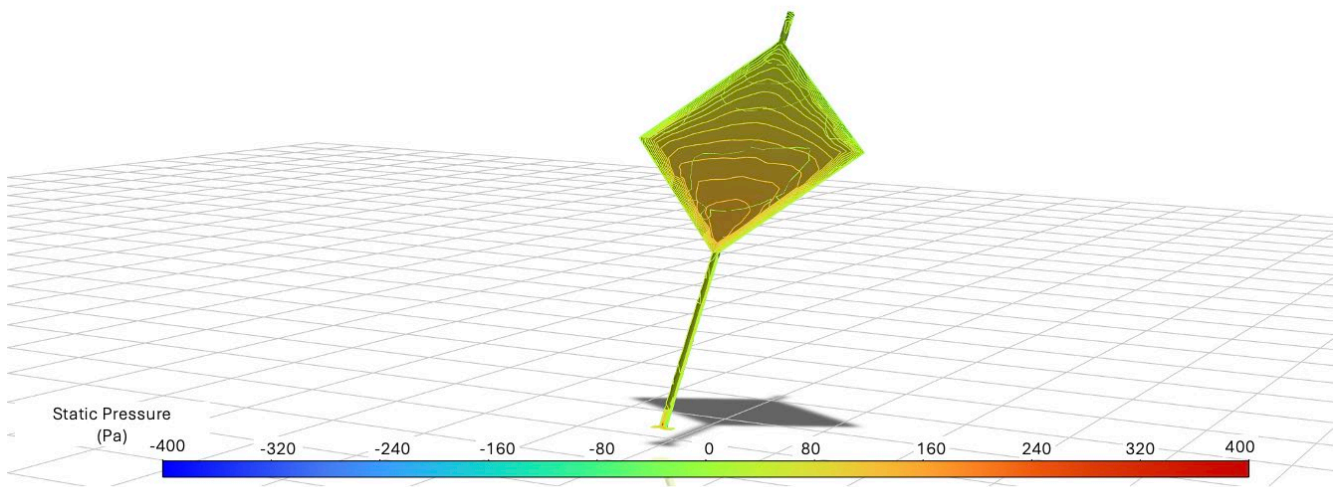
Figure 22. Illustrations. Structural finite-element mesh in ANSYS Mechanical 2025: (a) unstructured mesh with localized refinement near critical regions; (b) element quality distribution.

Load Transfer and Coupling Strategy

The CFD-FEA coupling was performed using a two-way FSI setup in ANSYS Workbench System Coupling. In two-way FSI, aerodynamic loads deform the structure, and that deformation is returned to the fluid solver so the flow field can evolve on the updated geometry. This feedback is important when structural motion alters local aerodynamics. In contrast, one-way FSI applies fluid loads to the structure without allowing the structural deformation to influence the airflow, which can lead to overestimated loads and responses in our case (Ansys Fluent User’s Guide, 2025).



(a)



(b)

Figure 23. Illustration. Instantaneous aerodynamic response of tilted temporary sign under wind loading: (a) velocity magnitude contours in the surrounding flow field; (b) static pressure contours on the sign surface.

At each time step, ANSYS Fluent computed the transient pressure distribution on the sign surface (or equivalent surface forces) and transferred these loads to ANSYS Mechanical. A time step of 0.005 s was selected to support stable convergence and to resolve the transient interaction, consistent with time-step limits governed by local flow speed and the smallest mesh length scale (i.e., a Courant–Friedrichs–Lewy–type criterion) (Ansys Fluent User’s Guide, 2025). The loads were mapped (Figure 23) onto the structural mesh while accounting for differences in mesh density and element formulation. ANSYS Mechanical then solved for the structural response (displacement, rotation, and stress) and returned the interface displacements to Fluent. Fluent used these displacements to update the fluid boundary through dynamic meshing and advanced the flow solution to the next time step. This exchange continued sequentially throughout the simulation. Figure 24 shows an algorithmic overview of System Coupling for two-way FSI in ANSYS Workbench.

Algorithm 1 Two-Way CFD–FEA Coupling

Require: CFD model in Fluent, FEA model in Mechanical, interface surfaces Γ , time step Δt , total steps N , tolerance ε , max coupling iterations I_{\max}
Ensure: Coupled time histories of interface loads/pressures and structural response displacement

- 1: Initialize ANSYS System Coupling; register Fluent and Mechanical participants
- 2: Define data transfers on Γ : *Forces* (CFD→FEA) and *Displacements* (FEA→CFD)
- 3: Initialize flow field and structural state; set initial interface displacement $u^0 = \mathbf{0}$
- 4: **for** $n = 1$ to N **do** ▷ Time marching
- 5: $k \leftarrow 0$
- 6: **repeat** ▷ Inner coupling iterations
- 7: $k \leftarrow k + 1$
- 8: **CFD solve (Fluent):** advance flow over Δt using current interface geometry $u^{n,k-1}$
- 9: Compute interface loads $L^{n,k}$ on Γ
- 10: **Transfer (CFD→FEA):** map $L^{n,k}$ from CFD surface mesh to structural interface mesh
- 11: **FEA solve (Mechanical):** solve for structural response under $L^{n,k}$ to obtain $u^{n,k}$
- 12: **Transfer (FEA→CFD):** map $u^{n,k}$ back to the CFD boundary on Γ
- 13: **Mesh update (Fluent):** update the fluid boundary using $u^{n,k}$ via dynamic meshing
- 14: **until** $\|u^{n,k} - u^{n,k-1}\| < \varepsilon$ **or** $k = I_{\max}$
- 15: **end for**
- 16: Post-process: maximum displacement, stress distributions

Figure 24. Illustration. Two-way coupling algorithm.

RESULTS

In this study, the primary outputs of the structural analysis include time-dependent tip displacement, with emphasis placed on the functional performance and visible motion of the sign system rather than on ultimate material failure. Therefore, the FEA results focus on wind-induced deformation and vibration behavior rather than sliding, uplifting, or overturning. To characterize the structural response, the tip displacement was converted into a tilting angle (i.e., rotation with respect to the vertical axis), as illustrated in Figure 25.

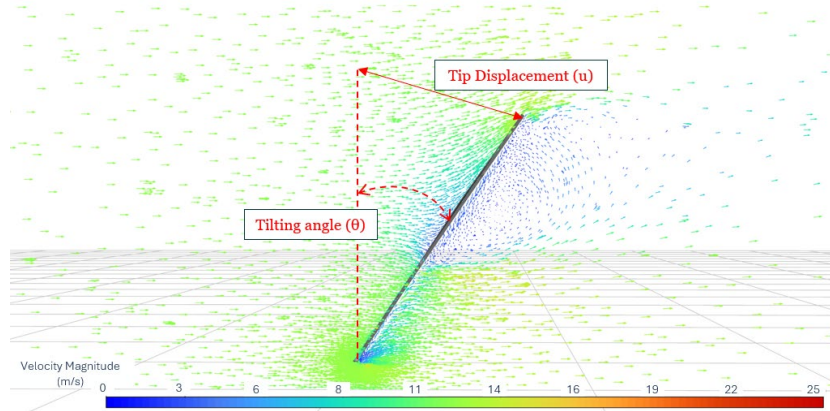


Figure 25. Illustration. Geometric interpretation of sign tip displacement and tilting angle.

Response Under Natural Gusty Wind Conditions

For the wind-only loading simulations, tip displacement values were evaluated for 20, 30, and 40 mph wind levels under the gust scenarios described in the Natural Gusty Wind section. These gust cases were classified by the rise time required to increase from 0 to 40 mph: 5 s for the slow-ramping case, 3 s for the moderate case, and 2 s for the impulsive case. This classification was used to compare the sensitivity of sign tilt to loading duration.

The simulations primarily modeled a 40 mph gust (Figure 26). For angle estimation, displacement values were extracted from the time-displacement history at the time when the wind speed crossed the selected threshold (e.g., 20, 30, or 40 mph). Because the gust speed increases continuously, the structural response may lag the instantaneous wind-speed threshold. Running separate simulations for each individual wind-speed level would be computationally repetitive and inefficient. Therefore, to maintain a practical and relatively simple approach while accounting for inertia-related dynamic effects, a conservative dynamic amplification factor (DAF) was applied to estimate the tilting angle from the time-displacement history response. Based on calibration from multiple simulation runs at different wind speeds, representative DAF ranges were adopted as approximately 1.1–1.3 for a slow-ramping gust, 1.3–1.7 for a moderate gust, and up to 1.8–2.0 for an impulsive gust. Accordingly, rotation-based responses were adjusted using: $\theta_c = \theta_s \times \text{DAF}$, where θ_c is the corrected tilting angle and θ_s is the computed tilting angle. Thus, the displacement at each wind-speed threshold-crossing time was first converted to an equivalent tilting angle and then multiplied by the representative DAF to account for transient lag and inertial amplification. This approach allowed the development of a practical comparative table without requiring additional simulations for each wind-speed stage or hold phase.

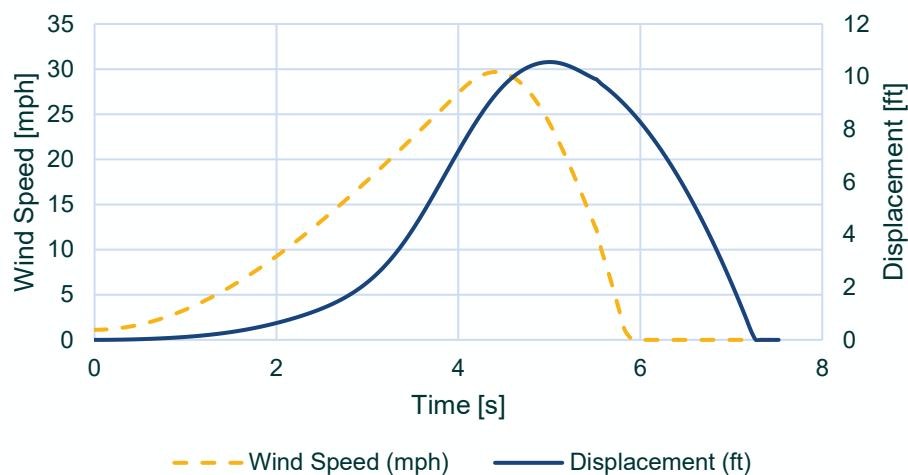


Figure 26. Graph. Time-displacement history plot of wind speed and sign tip displacement.

From the simulations, we found that although impulsive gusts are generally more severe in terms of acceleration, inertial force spikes, base reaction spikes, and vibration excitation, the development of tilt angle (i.e., displacement/rotation) typically requires time. As a result, a longer ramp duration can produce a larger displacement and tilting angle, even when associated with a lower DAF. For the

present sign model, the slow-ramping gust produced greater tilt because the longer loading duration allowed greater displacement buildup, whereas the impulsive gust primarily increased inertial demand but acted too briefly to generate the same peak rotation. Figure 27 shows the corresponding response trends: the time-displacement history and the displacement-velocity relationship under the applied wind loading.

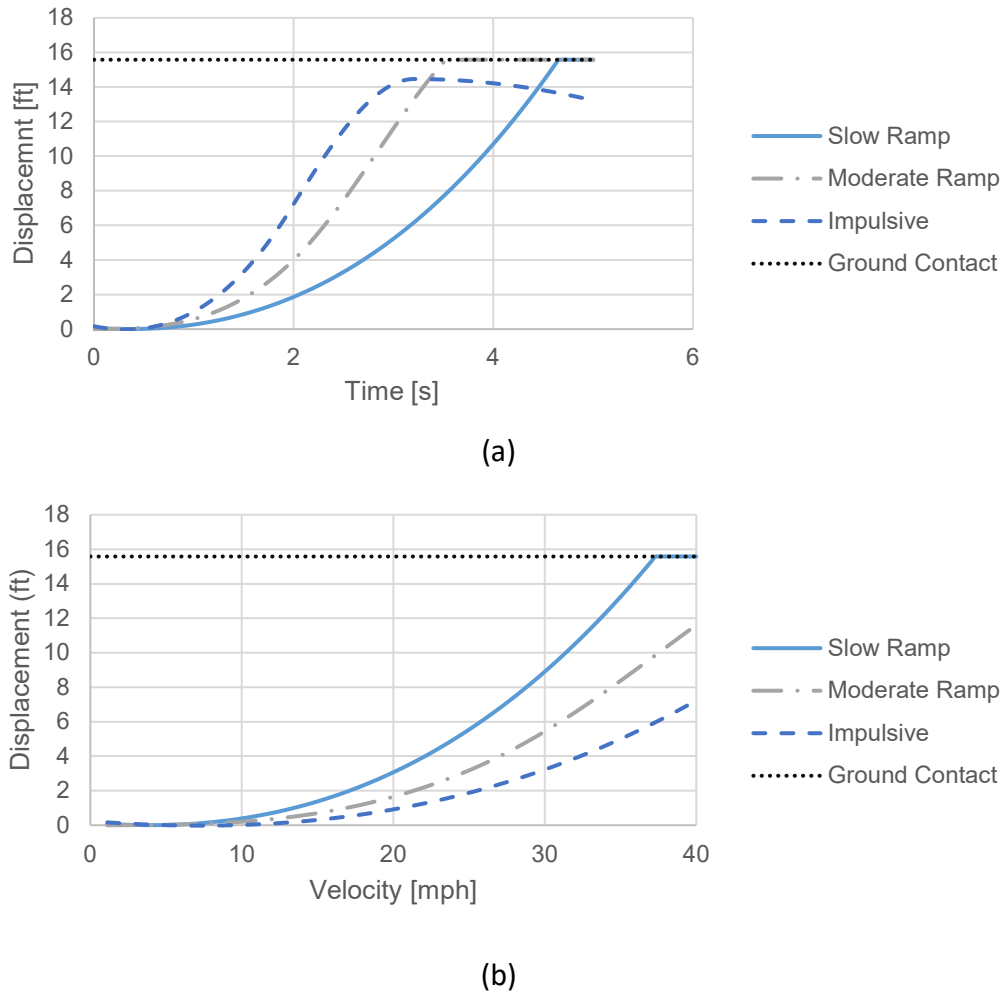


Figure 27. Graph. (a) Time-displacement response, (b) displacement-wind speed response for different gust loading patterns.

Response to Vehicle-Induced Wind Loads

The vehicle-induced wind-gust simulation was conducted only for the tall stand-mounted temporary sign plates. Based on the vehicle pass-by modeling framework described in the Truck-Induced Wind section, output displacements were estimated for two vehicle-induced loading cases: (i) the single-truck pass-by case and (ii) the three-truck platoon case. Figure 28 shows the pressure-time history for the sign along with three representative moments from the single-truck pass-by case. Three distinct pressure peaks can be seen, each corresponding to a different stage of the truck moving past the sign. These peaks occur because the airflow around the sign changes as the truck approaches, passes

alongside, and moves away. As the truck approaches the sign, pressure first builds up on the sign face, then quickly changes to suction as the truck wake passes. This short but sharp pressure change creates an impulsive aerodynamic load, which causes a noticeable lateral displacement peak, followed by gradually decreasing oscillations typical of a lightly damped flexible system.

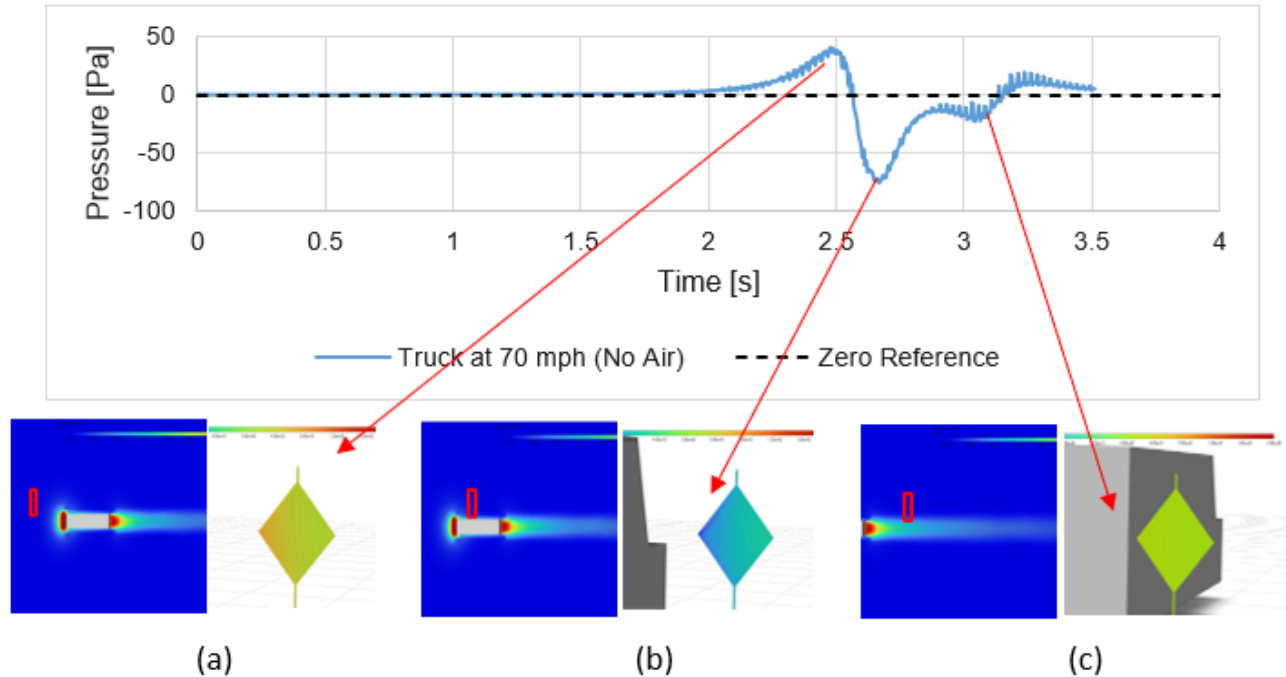


Figure 28. Graph. Pressure-time history and representative flow field at three characteristic instances of a single-truck pass-by event: (a) approaches, (b) passes alongside, and (c) moves away.

The displacement responses in Figure 29 show clear differences between the single-truck and three-truck platoon loading scenarios. In the single-truck pass-by case, the sign tip response is characterized by a short impulsive lateral displacement followed by rapidly decaying oscillations, reflecting the brief aerodynamic excitation generated by an isolated vehicle wake. In contrast, the three-truck platoon case can produce larger peak lateral displacements and a longer response duration because the sign is subjected to repeated pressure transients from successive vehicles.

The magnitude of the platoon response depends on the phase relationship between the incoming aerodynamic pulses and the ongoing structural vibration. When the loading from successive trucks arrives in a similar phase, the responses may combine constructively, leading to larger displacements. However, changes in bumper-to-bumper spacing or timing can shift the phase relationship, and partial cancellation may occur if the excitations arrive out of phase. In such cases, the peak tip displacement may be smaller than that of the single-truck case. In the present study, ambient wind was not included in the truck pass-by simulations to isolate the vehicle-induced effect and reduce computational cost. In practice, however, a truck platoon combined with background wind or a slow-ramping gust could create stronger or repeated excitations, which may increase the likelihood of temporary sign legibility issues.

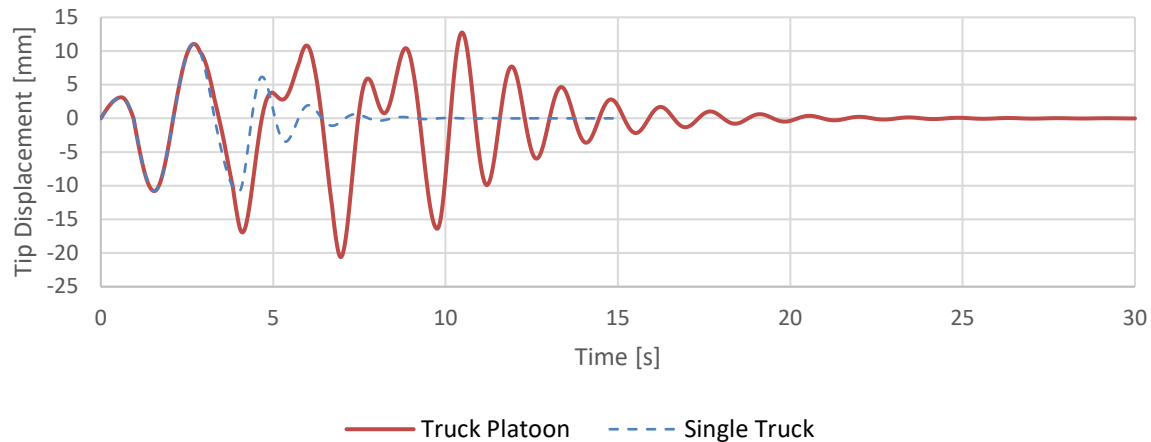


Figure 29. Graph. Time histories of tip displacement for the single-truck and three-truck platoon pass-by cases.

To make the motion more visible, Figure 30 shows the sign response at 10 times deformation scale for the single-truck case. Although the actual displacement is small and may be difficult to detect with the naked eye, the scaled view highlights the transient lateral sway and the short post-event oscillation that occurs immediately after the truck passes. These results suggest that vehicle-induced gusts, while brief, can still generate noticeable transient deflection and short-term vibration, which may temporarily reduce sign visibility and message readability even when overall structural stability is maintained.

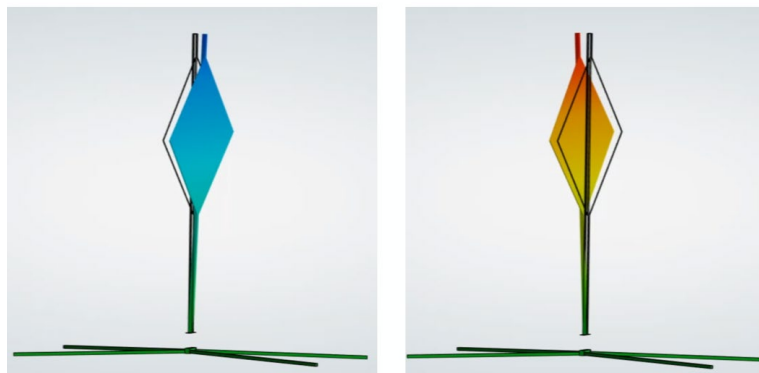


Figure 30. Illustration. Transient oscillatory motion snapshots of the temporary sign during a single-truck pass by (10x scaled).

Serviceability-Based Interpretation

To compare the performance of different temporary sign systems, the same general loading setup was applied to three sign configurations: tall post-mounted, short post-mounted, and tripod mounted. For the two flexible spring-supported post-mounted configurations, the same spring-base properties were used so that the effect of sign height could be compared directly. In these spring-supported systems, the main concern is not immediate structural failure, but rather oscillation and

rotation, which can reduce sign visibility and message readability at longer viewing distances. Although no widely accepted standard was identified for allowable traffic-sign tilt in relation to legibility, published guidance suggests that neighboring states (e.g., Indiana) may permit temporary mounted construction signs on tripod supports with tilt angles of less than 30° (INDOT, 2024). Based on this, rotations beyond this level may be considered a practical indicator of reduced far-field readability. In contrast, for the more rigid tripod-supported configuration, visible oscillation is less critical; instead, the primary concern is base sliding, ground movement, or overturning, especially when the sign is not properly ballasted.

Table 4 summarizes the finite-element simulation results for the different sign configurations under transient wind-loading conditions at peak gust speeds of 20, 30, and 40 mph. The results show that slower-ramping gusts can produce larger tilting angles because the load acts over a longer duration, allowing greater displacement to develop. For the same spring stiffness, the short post-mounted sign performs better than the tall post-mounted sign, exhibiting lower rotation under the same loading conditions. The tripod-mounted sign shows limited deformation response, but its stability becomes a concern: It may remain standing at lower wind speeds under some gust shapes, while at higher wind speeds it is more likely to overturn. Overall, the table highlights the trade-off between flexibility-related readability issues in spring-supported signs and stability-related overturning risk in tripod-supported signs.

Table 4. Summary of Corrected Equivalent Tilting Angles for the Modeled Temporary Sign-Stand Configurations under Different Transient Aerodynamic Loading Conditions

Sign Model	Wind Speed [mph]	Slow Ramp (θ_c)	Moderate Ramp (θ_c)	Impulsive (θ_c)	Single-Truck Response	Truck Platoon Response
Tall post-mounted	20	19.24°	12.91°	9.56°	2.73°	3.90°
	30	57.30°	42.93°	33.74°		
	40	≥ 90°	≥ 90°	76.76°		
Short post-mounted	20	17.97°	12.06°	8.93°	x	x
	30	40.83°	30.59°	24.04°		
	40	85.69°	58.34°	46.87°		
Tripod mounted	20	Standing	Standing	Overturned	x	x
	30	Overturned	Overturned	Overturned		
	40	Overturned	Overturned	Overturned		

CHAPTER 5: RECOMMENDATIONS

This research project completed three tasks. First, a literature and practice review was conducted to identify state-of-the-art deployment and design (function, equipment, and components) of temporary sign support systems. The literature focused on the use of temporary sign support systems and the effects of wind loads on temporary sign support systems. Second, a series of field experiments at test tracks in Illinois (including ICART and ICT) were conducted to evaluate the systems' responses to a passing truck and front-facing winds. Third, based on the temporary sign support systems' response to front-facing winds, a preliminary finite-element analysis was performed to evaluate the response of selected temporary sign support systems (tripod, short four-legged with springs, and tall four-legged with springs). The main findings can be summarized as follows:

- The different designs of temporary sign support systems have a central role in how they respond to winds; thus, the systems were organized into four groups depending on their height, number of legs, and use of springs.
- Rigid temporary sign support systems (those without spring-based support) tend to fail under moderate winds (4 or above on the Beaufort Scale), but the use of properly installed sandbags as ballasts improve their resilience (tested to gusts up to 7 on the Beaufort Scale without failing).
- Spring-based temporary sign support systems are less likely to fail, but sign visibility may be compromised if the springs are not stiff enough, due to large deflections from wind.
- Stiffer spring-based systems (e.g., dual-leaf spring supports) may still experience horizontal displacement, but they are less likely to fail.
- Shorter signs generally performed better than taller signs under the same spring stiffness. However, in practice, shorter signs may also use more flexible springs or lighter components.
- Slow-ramping or longer-duration gusts may produce greater deflection than short-duration gusts, because the structure has more time to build displacement under sustained loading.
- No significant deflection was observed from a single passing truck or even a three-truck platoon under no-wind conditions. However, vehicle pass-by loading may intensify sign oscillation when ambient gust wind is already present.

These findings are summarized in the deployment recommendations in Table 5, where each group of temporary sign support systems is labeled according to their performance under different wind loads. IDOT's districts can use this table in combination with Figure 1, where the expected maximum gust speed in each season and district is listed.

Table 5. Summary of Recommendations

Expected Maximum Gust Speed	Tripods	Small four-legged without springs	Small four-legged with springs	Tall four-legged with springs
< 10 mph	Safe to use	Safe to use	Safe to use	Safe to use
10 mph	Safe to use	Safe to use	Safe to use	Safe to use
20 mph	Requires ballasts	Requires ballasts	Safe to use	Safe to use
30 mph	Not recommended	Requires ballasts	Legibility issues	Legibility issues
≥ 40 mph	Not recommended	Not recommended	Not recommended	Not recommended

The proposed finite-element analysis framework provides a practical means to evaluate temporary sign support response under both natural wind and vehicle-induced aerodynamic loading. It also facilitates comparison of deflection angles and support reactions across spring-based systems with varying stiffness. Accordingly, the framework can serve as a useful analytical tool for future evaluation of temporary sign support performance under transient loading conditions. However, several limitations remain and warrant further study:

- The response of temporary sign support systems to non-front-facing natural winds needs further evaluation. Some temporary sign support systems position the signs at an angle to the ground, and their response to, for example, back-facing winds is still not clear.
- Although single- and multi-truck platoon pass-by cases did not produce significant responses on their own, their combined effect with background gust wind may lead to different and potentially more intense behavior.
- Spring stiffness and dampening ranges should be standardized to support more precise and comparable performance evaluation.
- Legibility-related safety risks of spring-based systems should be evaluated more thoroughly. Although these systems are less likely to fail structurally, wind-induced deflection may still reduce sign readability. Future work should establish practical readability criteria, including a maximum allowable tilt angle and a minimum viewing distance needed to preserve adequate driver reaction time.

REFERENCES

- American Association of State Highway and Transportation Officials. (2016). *Manual for assessing safety hardware* (2nd ed.). AASHTO.
- Ansys Fluent User's Guide. (2025). https://ansyshelp.ansys.com/Views/Secured/corp/v252/en/pdf/Ansys_Fluent_Users_Guide.pdf
- Bae, S.-W., Tate, D., Wood, T., Zuo, D., Bligh, R., Menges, W. L., Gonzalez, V., Griggs, D., & Yang, Q. (2014). *Testing of alternative supporting materials for portable roll-up signs used for maintenance work zones* (Report No. FHWA/TX-14/0-6639-1). Texas Tech University, Center for Multidisciplinary Research in Transportation. https://www.depts.ttu.edu/techmrtweb/documents/reports/complete_reports/0-6639_1_FINAL.pdf
- Barrero-Gil, A., & Sanz-Andrés, A. (2009). Aeroelastic effects in a traffic sign panel induced by a passing vehicle. *Journal of Wind Engineering and Industrial Aerodynamics*, *97*, 298–303. <https://doi.org/10.1016/j.jweia.2009.07.001>
- Center for Urban Transportation Research. (2007). Enhancing traffic signs to resist hurricane-force winds. University of South Florida Center for Urban Transportation Research
- Choose Energy. (2026). Wind Energy Generation by State. Accessed February 26, 2026, <https://www.chooseenergy.com/data-center/wind-generation-by-state/>
- Connecticut Department of Transportation, & Federal Highway Administration. (2017, December). *2017 Work Zone Safety and Mobility Process Review Final Report*. State of Connecticut Department of Transportation, Bureau of Engineering and Construction.
- Du, J., Qiao, F., Zhou, L., & Li, Q. (2020). Warrants and recommendations on using temporary work zone signs in high wind areas. In F. Qiao, Y. Bai, P.-S. Lin, S. I. J. Chien, Y. Zhang, & L. Zhu (Eds.), *Resilience and Sustainable Transportation Systems: Selected papers from the 13th Asia Pacific Transportation Development Conference* (pp. 186–195). American Society of Civil Engineers (ASCE). <https://doi.org/10.1061/9780784482902.022>
- Federal Highway Administration. (2023, December). *Manual on uniform traffic control devices for streets and highways* (11th ed.). U.S. Department of Transportation.
- Franke, J., Hellsten, A., Schlünzen, H., & Carissimo, B. (2007). *Best Practice Guideline for the CFD Simulation of Flows in the Urban Environment*. COST European Cooperation in Science and Technology. <https://hal.science/hal-04181390v1>
- Harwood, D. W., Glauz, W. D., & Mason, J. M., Jr. (1989). Stopping sight distance design for large trucks. *Transportation Research Record*, *1208*, 36–46.
- Illinois State Water Survey. (n.d.). Water and Atmospheric Resources Monitoring Program. Retrieved February 26, 2026, <https://www.isws.illinois.edu/warm/datatype.asp>
- Indiana Department of Transportation. (2024). *Standard specifications: Division 800—Traffic control devices and lighting (Section 801—Traffic controls for construction and maintenance operations)*. <https://www.in.gov/dot/div/contracts/standards/book/sep23/800-2024.pdf>

- Kumar, A. N., Guzzomi, A. L., Amoh-Gyimah, R., Ellis, P., & Wiseman, B. (2023). Understanding and improving temporary road sign stability. *Journal of Road Safety*, 34(1), 23–38.
<https://doi.org/10.33492/JRS-D-22-00037>
- National Highway Traffic Safety Administration. (2015). *Traffic safety facts*. National Center for Statistics and Analysis.
- Riley, P., & Soffian, S. (2017, Sept. 13). Hurricane Irma: Inoperable traffic lights are four-way stops. *Naples Daily News*. <https://www.naplesnews.com/story/weather/hurricanes/2017/09/13/hurricane-irma-inoperable-traffic-lights-four-way-stops/662150001/?gnt-cfr=1&gca-cat=p&gca-uir=false&gca-epti=z116480e116480v000088&gca-ft=179&gca-ds=sophi>
- Qiao, F., Du, J., Zhou, L., & Bakare, A. (2019). *Work zone materials for temporary signs in high wind areas: Final report* (Report No. FHWA/TX-19/0-6993-1). Texas Southern University, Innovative Transportation Research Institute.
- Sanz-Andrés, A., Santiago-Prowald, J., Baker, C., & Quinn, A. (2003). Vehicle-induced loads on traffic sign panels. *Journal of Wind Engineering and Industrial Aerodynamics*, 91, 925–942.
[https://doi.org/10.1016/S0167-6105\(03\)00035-7](https://doi.org/10.1016/S0167-6105(03)00035-7)
- Texas Department of Transportation. (2016). Texas Motor Vehicle Crash Statistics—2016. Accessed December 2, 2025, <https://www.txdot.gov/data-maps/crash-reports-records/motor-vehicle-crash-statistics/archive/2016-crash-statistics.html>
- Toy, N., Savory, E., & Akintaro, S. (1996). Wind loads on perforated flat plate temporary road signs. Proceedings of the BBAA3 Conference, Blacksburg, VA, USA.
- Weatherford, J. S. (2008). *Hurricane Ike traffic signal preparation & recovery*. Department of Public Works and Engineering.
- Washington Department of Transportation. (2015). *WSDOT traffic manual*. WSDOT.
- Zuo, D., & Letchford, C. W. (2010). Wind-induced vibration of a traffic-signal-support structure with cantilevered tapered circular mast arm. *Engineering Structures*, 32, 3171–3179.
<https://doi.org/10.1016/j.engstruct.2010.06.005>



I ILLINOIS